U.PORTO
FEUP FACULDADE DE ENGENHARIA
UNIVERSIDADE DO PORTO

Structural Analysis of a Freight Wagon

Ana Leonor de Oliveira Ribeiro

Thesis submitted to Universidade do Porto – Faculdade de Engenharia
in partial fulfillment of the requirements for the degree of
Master in Mechanical Engineering

Supervisores
Prof. Dr. Abílio de Jesus
Prof. Dr. Francisco Pires
Dr. Cláudio Horas

Mestrado em Engenharia Mecânica (M.EM)
Departamento de Engenharia Mecânica (DEMec)
Faculdade de Engenharia da Universidade do Porto (FEUP)

Abstract

Railways, which once had a major role in people and goods transportation, gradually lost importance as more competitive transportation methods emerged. However, in recent years, there has been a growing recognition of the advantages that an efficient and sustainable transport system, including railways, can offer. This renewed awareness has sparked a commitment to revitalise and modernise the railway sector, aligning with contemporary priorities for greener and more efficient mobility solutions. Recently, there has been a growing recognition of the need to invest in this industry, evidenced by the increasing number of projects in this field. This master's thesis aligns with the recent Smart Wagons project, which aims to develop a freight wagon designed for container transport, included in the Sggrss classification. The primary objective of this study, forming part of the initial phase of the project, is to construct and analyse a preliminary structural model of this wagon.

To achieve this goal, a geometric model was created based on an existing wagon design. Subsequently, finite element analysis (FEA) software was employed to conduct structural analysis. Six different load cases were considered, comprising two longitudinal load cases, two vertical load cases, and two more related to the superposition effect of those two types. This approach adheres to the stipulations outlined in the European standard, allowing for a comprehensive assessment of the wagon's structural response under various loading conditions.

This study encompasses three key aspects: static, fatigue, and modal analysis. The static analysis results were instrumental in identifying critical structural points. Subsequently, an evaluation was carried out to ensure compliance with the static structural requirements defined in the relevant standards. Following this, a comprehensive fatigue analysis was conducted, focusing not only on the overall underframe but also on the welded connections. It is worth noting that these numerous welded details in the wagon are of utmost importance due to the material used, which is mild steel S355, making fatigue analysis highly relevant. Lastly, the modal analysis allowed for an assessment of the wagon's dynamic properties, offering valuable insights for the planning of future dynamic and instability analyses.

Finally, the key findings from this research are presented. This study effectively fulfilled the static requirements, yet encountered non-compliance with fatigue criteria under different load cases and welding configurations. Furthermore, the document outlines intriguing avenues for future research and development in this domain, such as employing more detailed fatigue assessment methods like cumulative damage approach.

Keywords: Railways, Freight Wagon, Strength Analysis, Finite Element Method, Fatigue Analysis

Resumo

A ferrovia, que outrora desempenhou um papel importante no transporte de pessoas e mercadorias, foi gradualmente perdendo importância à medida que surgiam métodos de transporte mais competitivos. No entanto, nos últimos anos, tem havido um reconhecimento crescente das vantagens que um sistema de transportes eficiente e sustentável, incluindo os caminhos-de-ferro, pode oferecer. Esta consciência renovada desencadeou um compromisso para revitalizar e modernizar o sector ferroviário, alinhando com as prioridades actuais de soluções de mobilidade mais ecológicas e eficientes. Recentemente, tem havido um reconhecimento crescente da necessidade de investir nesta indústria, evidenciado pelo número crescente de projectos neste domínio. Esta tese de mestrado alinha-se com o recente projeto Smart Wagons, que visa o desenvolvimento de um vagão de mercadorias destinado ao transporte de contentores, incluído na classificação Sggrss. O objetivo principal deste estudo, que se insere na fase inicial do projeto, é a construção e análise de um modelo estrutural preliminar deste vagão.

Para atingir este objetivo, foi criado um modelo geométrico a partir de um de vagão existente. Posteriormente, foi utilizado um software de análise de elementos finitos (FEA) para efetuar a análise estrutural. Foram considerados seis casos de carga diferentes, incluindo dois casos de carga longitudinal, dois casos de carga vertical e mais dois relacionados com o efeito de sobreposição desses dois tipos. Esta abordagem obedece aos requisitos da norma europeia, permitindo uma avaliação alargada da resposta estrutural do vagão em várias condições de carga.

Este estudo engloba três aspectos fundamentais: análise estática, de fadiga e modal. Os resultados da análise estática foram fundamentais para identificar os pontos críticos da estrutura. Posteriormente, foi efetuada uma avaliação para garantir a conformidade com os requisitos estruturais estáticos definidos nas normas relevantes. Em seguida, foi efetuada uma análise de fadiga, centrada não só na estrutura geral, mas também nas ligações soldadas. É de salientar que estes numerosos detalhes soldados no vagão são de extrema importância devido ao material utilizado, que é o aço macio S355, tornando a análise de fadiga altamente relevante. Por último, a análise modal permitiu avaliar as propriedades dinâmicas do vagão, proporcionando informações valiosas para o planeamento de futuras análises dinâmicas e de instabilidade.

Finalmente, são apresentadas as principais conclusões desta investigação. Este estudo cumpriu efetivamente os requisitos estáticos, mas deparou-se com não conformidade com os critérios de fadiga em diferentes casos de carga e configurações de soldadura. Por fim, o documento apresenta hipóteses interessantes para investigação e desenvolvimento futuros neste domínio, como a utilização de métodos de avaliação da fadiga mais pormenorizados, como a abordagem dos danos cumulativos.

Palavra-chaves: Ferrovia, Vagão de Mercadorias, Análise de Resistência, Método de Elementos Finitos, Análise de Fadiga

"Just keep swimming."

Dory

Acknowledgements

Em primeiro lugar, gostaria de agradecer ao Professor Abílio de Jesus pela orientação, apoio e confiança depositada em mim ao longo deste período. Agradeço também pelas valiosas sugestões, pelo incentivo constante e por proporcionar as melhores condições para o meu trabalho.

Devo um agradecimento especial Claúdio Horas por toda a ajuda e disponibilidade fornecida durante a realização desta dissertação. Os seus conhecimentos e experiência em análise estrutural foram sem dúvida valiosos para a minha tese. Estou genuinamente grata pela paciência e assistência prestada.

Gostaria também de expressar o meu agradecimento aos restantes membros do projeto Smart Wagons, que me fizeram sentir parte da equipa. As vossas contribuições foram essenciais para o sucesso do meu trabalho.

Aos meus amigos de curso, por todo o companheirismo e bons momentos passados, um muito obrigada. Este mestrado foi superado em conjunto. Ana Ribeiro, agradeço do fundo do coração todas as palavras de carinho e motivação ao longo destes 2 anos, e espero que não nos confundam mais.

Um muito especial obrigado à Maria e ao meu colega António. O que projeto FEUP une, nunca se separa. Esta 'Mistelga' foi do melhor que a faculdade me trouxe, guardo com carinho todos os momentos que partilhamos. Para vossa sorte (ou talvez azar), vão continuar a ouvir-me por muito tempo.

Quero ainda agradecer à minhas companheiras do polo. São muitos anos a partilhar piscina, memórias, vitórias e derrotas. Obrigada por me darem vontade de ir treinar, mesmo depois dos dias cansativos. Não seria a mesma pessoa sem tudo o que este desporto me trouxe. À Ticas, obrigada por seres a minha irmã mais velha/madrinha mais louca e por todas as boleias de Faísca. Pipas, por seres o Shifu para o meu Po, por seres especial, muito obrigada.

Por último, mas não menos importante, agradeço à minha família e em especial, aos meus pais, pelo amor incondicional, apoio, orientação e por tudo o que fazem por mim. E pai, quem diria que depois de tantos anos a ouvir-te falar de comboios, ia acabar a fazer uma tese sobre eles.

A todos os que me acompanharam, muito obrigada,

Leonor Ribeiro

Institutional Acknowledgements

This work is a result of Agenda "SMART WAGONS – Development of Production Capacity in Portugal of Smart Wagons for Freight", nr. C644940527-00000048, investment project nr. 27, financed by the Recovery and Resilience Plan (PRR) and by European Union - NextGeneration EU.

Contents

List of Figures

List of Tables

Chapter 1

Introduction

This introduction provides a comprehensive exploration of the background and underlying motivations that have propelled the creation of this dissertation (Section 1.1). It delineates the precise objectives that have guided the execution of the research (Section 1.2). Moreover, it outlines the structural framework that has been adopted throughout the various chapters comprising this document (as elaborated upon in Section 1.3).

1.1 Background

The transportation of goods plays a pivotal role in nations' economic growth and development. In recent decades, the landscape of freight transportation in Europe has witnessed a significant shift from rail to road as the preferred mode of transportation. Some factors, such as flexibility and shorter end-to-end times, have primarily driven this transition. However, the dominance of road transportation has brought along environmental concerns due to its higher pollution levels compared to railway transportation. In fact, rail transport only accounts for 0.4% of GHG emissions in the EU, despite making up 8% of passenger and 19% of freight transport in Europe [1], as can be seen in figure 1.1.

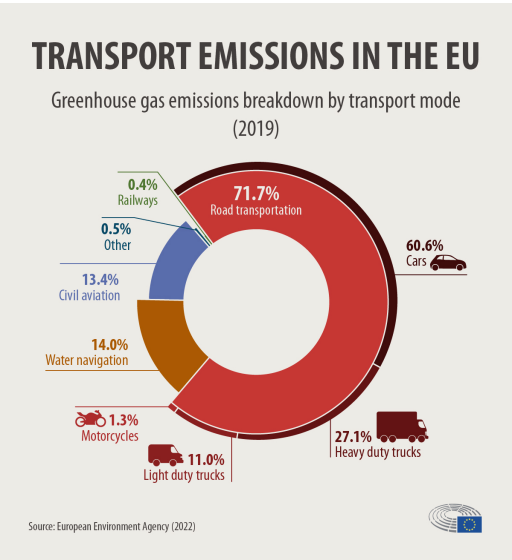

Figure 1.1: Transport emissions in the EU [2].

1.1. Background

Recognising the urgent need for a greener and more efficient freight transportation system, Europe has embraced the goal of promoting railway freight transportation as a viable solution. This objective has been further emphasised by the European Union's White Paper on Transport in 2019, which outlines comprehensive guidelines for achieving sustainable and efficient transportation throughout the European region. The White Paper sets a challenging target of achieving climate neutrality by 2050 and states that a significant portion of the current 75% of inland freight, currently carried by road, should shift to rail and inland waterways [3].

Various challenges must be addressed to attain these goals, including railway interoperability. In the European Union context, it was crucial to create a functional network to establish seamless physical links between the different countries, thus strengthening political cohesion. This initiative led to the creation of the Trans-European Transport Network (TEN-T), as depicted in figure 1.2. The TEN-T is vital for developing a coherent, efficient, multimodal, and high-quality transport infrastructure across the EU.

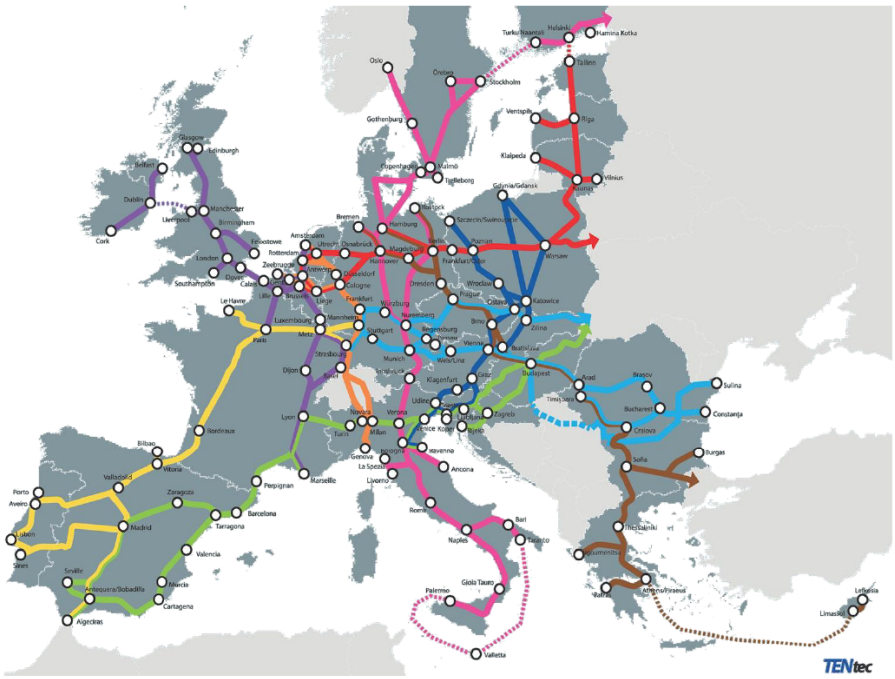

Figure 1.2: Trans-European Transport Network [4].

This network encompasses railways, inland waterways, short sea shipping routes and roads, all interlinking urban nodes, maritime and inland ports, airports, and terminals. It not only facilitates the efficient transportation of both people and goods but also ensures accessibility to jobs and services while fostering trade and economic growth. By eliminating physical gaps, bottlenecks, and missing links, the TEN-T strengthens the EU's economic, social, and territorial cohesion while creating integrated and seamless transport systems across borders. Furthermore, it places a strong emphasis on reducing the environmental footprint of transportation and enhancing network safety and resilience, aligning with the EU's broader sustainability objectives.

To achieve this transition, significant investments are required to enhance both infrastructure and vehicle capabilities. Upgrading existing rail networks, building new intermodal terminals, and developing advanced freight wagons are key aspects that demand attention. With this in mind, over the years, numerous projects have fostered innovation and facilitated the shift from rail to road transportation in Europe's freight industry.

One example is the Shift2Rail project, which focused on doing research and innovation and commercial products, increasing the integration of innovative and advanced technologies into new solutions for the railways. By bridging the gap between research and practical application, Shift2Rail aims to facilitate the rapid adoption of advanced technologies, ultimately leading to a more modern, efficient, and environmentally friendly European rail transportation system [5].

This thesis is a result of the Agenda "SMART WAGONS – Development of Production Capacity in Portugal of Smart Wagons for Freight", nr. C644940527-00000048, investment project nr. 27, financed by the Recovery and Resilience Plan (PRR) and by European Union - NextGeneration EU. The main objectives are to revive the railroad industry in Portugal and produce and maintain interoperable rail vehicles for freight transport in the European area, equipped with digital technology to optimise maintenance and operation, increasing their availability and improving the economic and environmental sustainability of the railroad.

These freight wagons carry heavy loads, subjecting them to substantial static forces. Consequently, they must possess enough strength to withstand these loads while being lightweight to ensure optimal energy consumption.

A critical factor in designing these wagons is the significant weight differential between their loaded and unloaded states. This variance has profound implications, especially for the wagon's suspension system, which must be finely tuned to accommodate this weight fluctuation.

Furthermore, these wagons are exposed to various dynamic load scenarios, encompassing the loading and unloading processes and the vibrations induced by the track. These dynamic forces are paramount in evaluating these vehicles' fatigue endurance. Given that these wagons are constructed through welding processes, a meticulous examination of their welded sections, particularly concerning fatigue resistance, becomes imperative.

The finite element method emerges as a pivotal tool in the contemporary freight wagon design landscape. Through simulations, this method not only expedites the design process but also economises time and costs. It facilitates structural optimisation by scrutinising simulation results, allowing for the identification of areas experiencing minimal stress levels.

This optimisation process holds profound significance. By reducing wagon weight, many advantages ensue, including decreased quantity of raw material, diminished energy consumption, reduced CO2 emissions, and increased load capacity. The latter, in particular, enhances the revenue potential for transportation companies. Ultimately, this approach contributes to the overarching goal of enhancing the sustainability of the railway industry, aligning perfectly with the objectives set forth in the first section of this introduction.

1.2 Objectives

The main objective of this dissertation is to develop a preliminary model of a freight wagon envisioned for the Smart Wagons project and perform a structural analysis. This shall be achieved by constructing a finite element model and comparing the results obtained with the structural requirements stipulated in the relevant standards. The main milestones of the present work are:

- Constructing a realistic model to obtain an accurate representation of the wagon for the finite element model;
- Evaluate the structural integrity by employing a static, fatigue and modal analysis.

In terms of methodology to accomplish these objectives, it is listed below tasks to be carried out throughout the dissertation development:

- Literature review on freight wagons, their characteristics and the different systems and mechanisms integrated into them;
- Brief literature review of Finite Element analysis practices in the design and study of freight wagons;
- Brief literature review about the regulatory environment surrounding this subject;
- Construction of the 3D model;
- Structural analysis of the wagon using the Finite Element Method.

1.3 Outline

In sequence with the previous sections, a brief description of the chapters found in this document is detailed in this section. Overall, the present dissertation is organised in five chapters. After the introductory chapter, the structure of this thesis is as follows:

Chapter 2 - State-of-the-art review

This chapter provides an in-depth exploration of the freight wagon topic. It begins with a general introduction to the characteristics of these vehicles. Subsequently, it delves into different categories of wagons and presents the systems constituting these vehicles, such as the running gear and coupling mechanisms. The chapter also highlights the significance and application of the Finite Element Method (FEM) in the design of these vehicles, referencing relevant studies and articles in this field. Finally, it offers a brief overview of the regulatory framework that governs these vehicles.

Chapter 3 - Case Study - Sggrss Wagon

This chapter is dedicated to presenting the case study of this project, which is the Sggrss wagon. It provides a detailed description of the geometric model and proceeds to elucidate the characteristics of the FEM model. Essential details such as meshing, applied boundary conditions, and the various load cases considered in the analysis are explained in this section.

Chapter 4 - Structural Analysis

Chapter 4 is dedicated to the analysis of the results extracted from the FEM model. It is divided into three parts. The first part covers static analysis, presenting the applied methodology and discussing the results. It assesses whether the structural requirements mandated by the relevant standards are met. The subsequent section is devoted to fatigue analysis, outlining the methodology and conducting an in-depth analysis of the results, with a particular focus on welded connections. Lastly, the chapter presents the outcomes of modal analysis, showcasing the vibration modes and explaining their behaviour.

Chapter 5 - Conclusions and Future Work

In this final chapter, the thesis concludes with a synthesis of the key findings and pertinent observations. Recommendations for future work and ongoing research directions in the realm of this thesis topic are also addressed.

1.3. Outline

Chapter 2

State-of-the-art review

This chapter offers a comprehensive exploration of the freight wagon domain. It starts with a broad introduction to the fundamental features of these vehicles. Subsequently, it delves into diverse wagon classifications and elucidates the intricate systems that compose these vehicles, encompassing components like the car body, running gear and coupling and braking mechanisms. Moreover, this chapter underscores the pivotal role of the Finite Element Method (FEM) in shaping the design of these wagons, substantiating its relevance with citations from pertinent research and articles. Concluding this chapter is a succinct overview of the regulatory framework that exerts control over these freight vehicles.

2.1 Freight Wagons

Freight wagons, also known as freight cars or goods wagons, are unpowered railway vehicles designed for a wide range of cargo transportation, such as raw materials, finished products and bulk goods. These indispensable elements of the rail transport system are available in diverse types and designs, tailored to accommodate various types of cargo. This review aims to explore these vehicles' fundamental features and functionalities, with a particular emphasis on the different systems that constitute them, such as the running gear, brake system, coupling mechanism, and other essential components. Subsequent sections will delve into these systems in more detail, providing a comprehensive understanding of the vital aspects of freight wagon technology and operations.

Two of the most relevant specifications for freight cars are the axle load and maximum design speed. Axle load refers to the weight transmitted by a single wheelset to the tracks, and the maximum design speed, commonly under 100 km/h in Portugal, correlates inversely with the axle load – higher axle loads correspond to lower design speeds. For instance, a wagon with an axle load of 22.5 tons cannot exceed 100 km/h, while one with a lower axle load of 20 tons can attain 120 km/h. Additional characteristics include the tare mass, which denotes the empty wagon weight, and the fully loaded mass, consisting of the empty vehicle mass plus its cargo. The latter must not surpass the designated axle load. Striking the right balance between mass and volume carrying capacity is pivotal for optimizing wagon efficiency [6].

The number of axles in freight wagons is a crucial parameter for characterizing these vehicles and plays a significant role in their operational capabilities. Figure 2.1 visually demonstrates various configurations of wagons based on their number of axles. This characteristic provides

valuable insights into the wagon's load-bearing capacity, stability, and distribution of cargo mass. Common examples include wagons with two axles, four axles (comprising two bogies, each with two axles), or even three bogies for articulated vehicles. Additionally, in cases where there is a need to distribute higher cargo mass while adhering to axle load limits, bogies can be constituted by more than two axles [6].

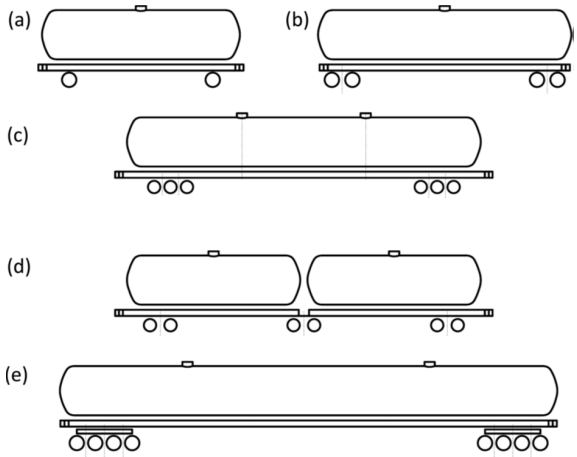

Figure 2.1: Types of rail vehicles by the number of axles: (a) 2-axle vehicle, (b) 4-axle vehicle with two 2-axle bogies, (c) 6-axle vehicle with two 3-axle bogies, (d) 6-axle articulated vehicle with three 2-axle bogies and (e) 8-axle vehicle with two 4-axle bogies [6].

Freight trains are composed of several freight wagons and a locomotive. The maximum length of the train is dictated by the traction capacity of the locomotive, as well as the railway's topography, like rail curvatures, and the overall weight of the train (locomotive + wagons). In Portugal, the train cannot surpass 750 m. While the traction force is only produced by the locomotive hauling the cars, the brakes are applied to each vehicle [6].

Regarding the geometry of the railway vehicles, some essential dimensions are explained below and illustrated in figure 2.2.

- **Vehicle wheel base**: The longitudinal distance between the outer bogies' centre or the vehicle's suspension. Additionally, for articulated wagons, the distance between neighbouring bogies is called section wheelbase [6].
- **Length between coupler axes**: The measurement of a wagon's length within a train, or the space it occupies, is determined between the axes of its coupling devices. The maximum length of four-axle vehicles between coupler axes is set to 25 m to ensure safety when curving [6].
- **Car body length**: This measurement represents the utmost length along the railway track. Generally, it corresponds to the distance between end beams, although certain wagon variations possess an extended upper section, enhancing the loading volume [6].
- **Coupler height**: This parameter is responsible for ensuring the coupling's safety and avoiding disconnection when the train is traversing uphill or downhill sections of the track [6].
- **Clearance diagram/Loading Gauge**: This diagram outlines the allowable space envelope around the railway track to accommodate the safe passage of trains through various structures, such as tunnels, bridges, and platforms. The loading gauge sets the maximum height, width, and depth dimensions for trains, preventing collisions with obstacles along the track and maintaining operational safety. This diagram also accounts for rail vehicles' potential

swaying like overhang on curves, hence, a kinematic and dynamic envelope are outlined. Furthermore, it is important to note that these measurements can vary between countries to suit specific conditions. An example of a general illustration this diagram is presented in figure 2.3.

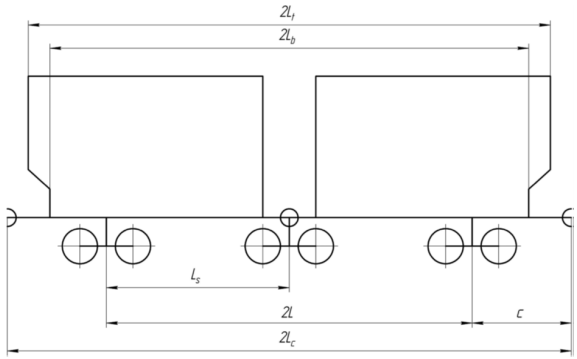

Figure 2.2: Articulated wagon measurements: $2L$ – vehicle wheelbase, L_s – section wheel base, $2L_c$ – length between coupler axes, $2L_b$ – length between end beams, $2L_t$ – length of the car body and C – length of the cantilever part [6].

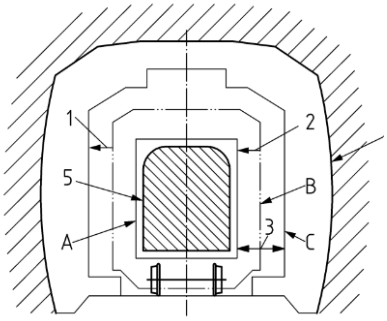

Figure 2.3: General illustration of the gauges [7].

2.1.1 Classification

Freight wagons exhibit a significant diversity in car body shapes, leading to their classification based on this characteristic. The categories include covered, flat and low-sided wagons, tank wagons, wagons of special construction, high-sided, discharging and refrigerated wagons. In the upcoming section 2.1.2, a more detailed description of each type will be made, highlighting their respective features and examples.

To ensure a standardized classification, a unified format for wagon coding, including letter and numeric identifiers, was established for all members of UIC. This classification is based on their specific operational applications. Following particular rules, the letter markings contain vital information: the first capital letter denotes the wagon's basic type designation (see table 2.1), while subsequent lower-case letters provide further details regarding technical and operational characteristics, known as additional letter type designations. For instance, the letter 's' indicates a maximum speed of 100 km/h, while 'ss' denotes a speed limit of 120 km/h. The definition of these letter markings is outlined in the Commission decision on the technical specification of interoperability related to the subsystem "Operation and management of transport" of the trans-European conventional railway network, as specified in the Interoperability Directive 2015/995/EC [8].

Table 2.1: UIC wagon classification.

Class	Wagon Type
G	Ordinary covered wagon
H	Special covered wagon
K	Ordinary flat wagon with separate axles
O	Open multi-purpose wagon (composite open high-sided flat wagon)
R	Ordinary flat wagon with bogies
L	Special flat wagon with separate axles
S	Special flat wagon with bogies
Z	Tank wagon
U	Special wagons
E	Ordinary open high-sided wagon
F	Special open high-sided wagon
T	Goods wagon with opening roof
I	Refrigerated van

Wagon numbers play a crucial role in railway operations, ensuring the correct identification of each railway wagon and facilitating effective communication between railway operators, infrastructure companies, and state authorities. The code is composed of 12 digits, where the first two indicate the type of vehicle and interoperability capacity, the next two digits are the country code where they operate, digits 5-8 refer to the vehicle type, digits 9-11 are the serial number and the last one is a self-check digit.

Figure 2.4 exhibits an example of the number inscription on a flat wagon and its classification (Sggrss).

Figure 2.4: Inscription on a flat wagon of class Sggrss.

2.1.2 Car Bodies

The various types of car bodies found in freight wagons are discussed in the following section. These wagons come in diverse designs, specifically tailored to meet the requirements of different types of cargo. The review includes covered, flat, tank, special construction wagons, high-sided and refrigerated wagons, each possessing unique features and functionalities. Notably, the study of the interaction between cargo and the car body plays a crucial role in vehicle dynamics research,

further emphasizing the significance of understanding how these wagons function and interact during transportation.

- **Covered wagon**

A covered wagon is a type of freight wagon designed with a roof and sidewalls to provide enclosed protection for the goods being transported. The primary purpose of a covered wagon is to safeguard the cargo from external elements such as rain, snow, dust, or direct sunlight during transportation. These wagons constitute a significant part of wagon fleet in Europe [9]. An example of a covered wagon can be seen in figure 2.5.

The box car body design resembles a box beam, where the load exerted on the floor causes bending, akin to a beam supported on two points. In this analogy, the floor and underframe can be likened to the bottom flange of the beam, while the side walls, functioning as the webs, bear the shear forces. Finally, the roof behaves similarly to the upper flange of the box beam [6].

Developing enclosed body designs poses several significant challenges, including addressing wide sliding door openings, ensuring the protection of the lightweight floor decking to prevent cargo damage during transit, and effectively withstanding concentrated loads from loaders [6].

Figure 2.5: Covered wagon - Gbs [10].

- **Flat Wagon**

Flat and low-sided wagons form the most extensive group of freight wagons, catering to a diverse range of cargo transportation needs. These versatile vehicles are designed to carry long elements, bars, rolled steel bands, timber, flat materials, bulk substances, containers, swap bodies, and even cars. They consist of an underframe and, in some designs when required, end walls, low-sided walls, stanchions and cargo security devices (ex: spigots). In summary, they offer flexibility and efficiency in transporting a vast array of goods [9]. Figure 2.6 illustrates a flat wagon for container transport and some of the mentioned attachments are presented in figure 2.7.

The underframe features two key components: the main longitudinal beams. These beams are arranged in two primary configurations. In the first setup (case a) of figure 2.8), the girders are positioned close to the wagon's centreline, spaced slightly apart, aligning with the longitudinal beams in the coupler area. Then, smaller-height beams are located on the side, supported by cantilevers extending from the girders. These hold the spigots, in the case of container transport, or different attachments. In the other configuration (case b) of figure 2.8), the main longitudinal beams are positioned on the outside and are interconnected by transversal beams, directly supporting the attachments [11].

The loading gauge limits the maximum height of the cargo area. To meet this requirement, it is advantageous to maintain a low underframe upper surface height. Thus, the height of the girders is extended downwards in areas not affected by the bogie. In the areas where the running gear is situated, the height of the beam faces limitations, which can pose challenges in attaining the necessary structural rigidity and strength for the vehicle. To overcome these issues, intricate beam

designs are developed, incorporating variations in plate thickness [6]. This effect is noticeable in the wagon examined within this study.

Figure 2.6: Flat wagon - Laagrss.

(a) Wagon with stanchions

(b) Spigot

Figure 2.7: Wagon attachments.

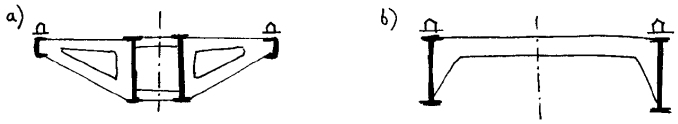

Figure 2.8: Positioning of girders [11].

- **Tank Wagons**

As the name implies, these wagons are outfitted with a tank for fluid transfer. The tank body is made up of a hermetically sealed cylindrical vessel that securely holds the products, as well as an underframe or two half-frames that allow load transfer from couplers and undercarriages to the wagon.

The transported cargo falls into distinct categories, which include cargoes transported under pressure, such as compressed gas; cargoes unloaded under pressure, like acids and chemical products; and cargoes transported and unloaded in unpressurised conditions, such as oils. The nature of the products heavily influences the choice of vessel material and its thickness. For instance, when dealing with corrosive fluids, a corrosion-resistant vessel becomes imperative to ensure safe transportation [9].

The tank's volume, payload capacity, permissible pressure, material, and design of the loading/discharge fitting are the key functional parameters of the tank that determine the feasibility and effectiveness of carrying one or more items.

The most challenging aspects of designing a tank car are increasing the volume of the vessel while working with a constrained clearance diagram and car length, minimising its weight, and ensuring the vessel's strength and fatigue resistance at attachment points on the underframe and in the hatch area [6]. Figure 2.9 presents an image of a tank wagon.

Figure 2.9: Tank wagon [12].

- **Wagons of special construction**

The design of U-type wagons is very diverse because they are special construction wagons that do not fall under any other type. However, they are typically deep-well wagons for transporting very heavy cargo or wagons with vessels for transporting freely loaded powder substances with pressure discharging [9]. An example of a special construction wagon is presented in figure 2.10.

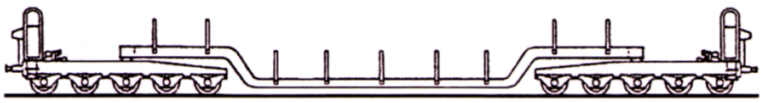

Figure 2.10: Uaai - Special 10-axle bogie deep-well wagon [9].

- **High-sided and discharging wagons**

The high-sided and discharging wagons encompass various types of open wagons designed for specific transport requirements. These wagons can have standard construction with a firm floor, high-side walls, and end walls, allowing for easy loading and unloading of bulk cargo. Some wagons within this group have discharging capabilities, with the unloading method specified in the wagon marking, for example discharging hatches on the bottom floor. Additionally, wagons with scrolling, foldable, tilting, or moving roofs offer versatile cargo handling options [9]. In figure 2.11, a hopper wagon is shown.

Figure 2.11: Hopper wagon - Tadns [13].

- **Refrigerated and Isothermal wagons**

Refrigerated and isothermal wagons are specialised freight wagons designed to maintain specific temperature conditions for the transported products. Refrigerated wagons are fitted with refrigeration units to maintain a controlled and low-temperature environment, ensuring the preservation

of perishable goods, such as food and pharmaceuticals. On the other hand, isothermal wagons do not have refrigeration. They are insulated, allowing the regulation of the internal temperature and providing a stable climate suitable for transporting goods that require protection from extreme temperature fluctuations [9].

2.1.3 Wagon Frames

The underframe is a critical structural component of freight wagons, providing the foundation for the entire vehicle. They are designed to withstand the weight of the cargo and the forces encountered during transportation and transmit longitudinal forces from one wagon to the adjacent ones in the train. The frame typically consists of longitudinal and transverse beans welded together to form a rigid structure.

Its primary purpose is to distribute the load evenly across the entire vehicle, ensuring stability and safety during operation. The main girders are continuous beams that run along the wagon's length, while the transverse members connect the longitudinal ones, providing lateral support and preventing excessive bending or twisting.

These structures are typically constructed of structural steel since it keeps costs low, is easy to manufacture and has good fatigue resistance. Nonetheless, there is a tendency to produce modern ones from high-strength steel, providing a balance of strength and weight, which helps to maximise the payload capacity while maintaining the required structural integrity.

When designing the wagon's frame, it is critical to consider the maximum longitudinal, vertical, and lateral forces experienced during regular haulage and shunting operations. This process must also be influenced by other factors regarding the type of cargo being transported, operating conditions and the wagon's purpose.

At last, proper maintenance and inspection of wagon frames are crucial to ensure their longevity and safe operation. Regular inspections help identify any signs of wear, damage, or fatigue, allowing for timely repairs or replacements [14].

2.1.4 Running gear/Bogie

The railway track's guidance mechanism is the fundamental differentiating characteristic that distinguishes railway vehicles from other wheeled transportation. The rails are in charge of not only supporting the wheels but also controlling their movement, establishing the direction of motion of the vehicle [6].

The running gear is a crucial system responsible for ensuring the safe motion of a railway vehicle along the track. This system comprises wheelsets with bearings, suspension elements and a braking system. Its main functions are the following:

- Transferring the vertical forces from the wheels to the railway;
- Guaranteeing the effective braking of the vehicle;
- Absorbing vibrations due to track landscape and irregularities;
- Guiding the wagon along the path.

One essential element of the running gear is the wheelsets (see figure 2.12), which consist of the wheels and the axles. The wheels are designed to withstand the substantial loads carried by

freight wagons and provide smooth rolling contact with the track. The axles serve as the rotational axis for the wheels and are housed within axle boxes, providing bearing support and allowing for controlled movement [6]. The remaining components, such as the suspension and braking system, will be addressed later.

Figure 2.12: Wheelsets [15].

Regarding running gear for railway wagons, two main options are available: single axles or bogies. In the former, there is only one axle at each end of the wagon, with all components mounted directly on the wagon body. A typical example of this is the "single-axle running gear with link suspension" (figure 2.13a). This mechanism is quite simple and lightweight, thereby maximising the wagon's payload [16]. However, this configuration poses limitations during curving, as the forces generated are high, restricting track curvatures and reducing wagon length [6, 17].

To address this issue, bogies are introduced as a solution. Bogies are subassemblies with two or more axles connected to a separate frame that rotates relative to the wagon frame, enabling greater curving capability. The connection is achieved through a centre-pivot that allows these rotations and two side-bearers that also act as static support for the car body and roll stiffness [16]. The bogie frame efficiently transmits all the longitudinal, lateral, and vertical forces between the car body and the wheelsets, ensuring smoother navigation along the tracks [6]. A commonly used bogie in freight wagons is the Y25 bogie (figure 2.13b), which has a steel frame in H form and has coil springs suspension.

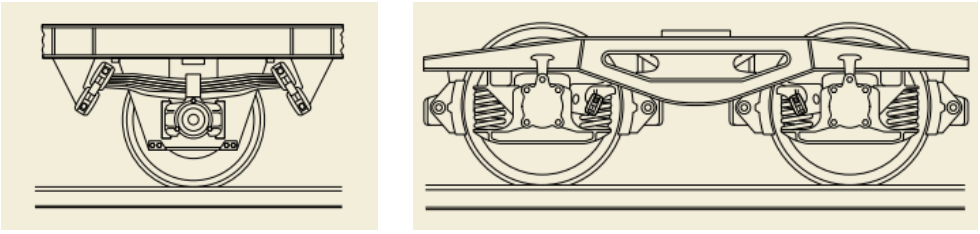

(a) Single-axle running gear with link suspension

(b) Y25 bogie

Figure 2.13: Running gear [18].

Efficient running gear and bogies are vital for various reasons. They reduce friction between the wheels and the tracks, minimising wear and tear and lowering maintenance costs. Additionally, well-designed bogies improve the wagon's stability during acceleration, deceleration, and cornering, ensuring safer and more reliable freight transportation [6].

The selection and design of running gear and bogies are critical factors for freight wagons, as

they directly impact the overall performance and safety of the railway system. Several crucial parameters come into play during this process [6]:

1. The track gauge must correspond to the railway's gauge and provide suitable wheelsets for smooth and stable operation.
2. The axle load and design speed have to be taken into consideration to ensure the compatibility of the bogie with the intended vehicle.
3. The bogie wheelbase plays a vital role in distributing the wagon's mass effectively along the track, impacting the bearing capacity of bridges and overall track stability.

These factors, along with other operational requirements and track conditions, collectively influence the optimal design and maintenance of running gear and bogies, ensuring the freight wagon fleet's efficiency, safety, and longevity.

2.1.5 Suspension

The suspension system of freight wagons (see figure 2.14) is located in the running gear and it is critical for providing support, stability, and smooth movement during rail transportation. Their elements can be classified as primary or secondary based on their location, connection and function.

The primary suspension is directly connected to the wheelsets and consists of spring and damper components between the bogie and the wheelset. This arrangement ensures stable running behaviour, low track forces, minimal wear, and excellent performance during curves [14]. It mainly isolates the bogie from short wavelength irregularities [19].

On the other hand, the secondary suspension is not connected to the wheelset and is usually interlinked with the car body and bogie. Traditionally known as bolster springs, these secondary suspension elements aim to isolate the car body from excitations transmitted from track irregularities via the wheelsets and bogie frames [14].

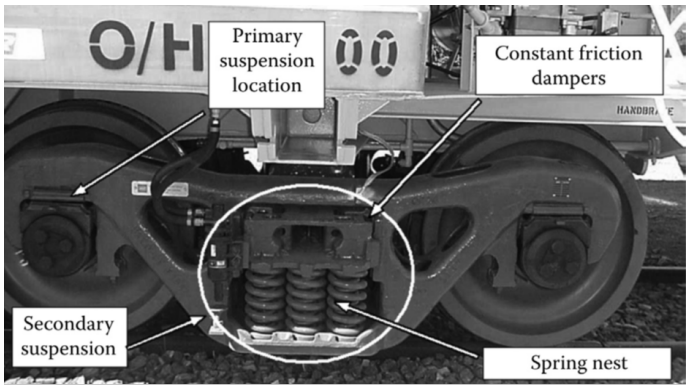

Figure 2.14: Example of a bogie's suspension system [14].

In most cases, springs are the preferred choice for suspension systems (as it is pointed in figure 2.14), commonly utilising coil or flat springs. However, modern bogie designs may incorporate alternative options like rubber, compressed airbags, or hybrid combinations, especially for passenger wagons [20]. Some examples are presented in figure 2.15.

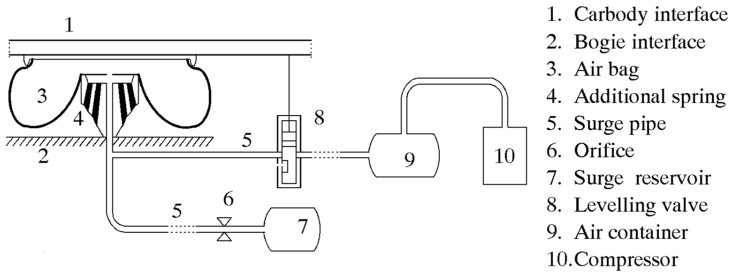

Figure 2.15: Air spring system [20].

As for damping functions, they are typically achieved through either friction or hydraulic devices. Some elastic elements, such as leaf springs, possess enough internal friction damping, negating the need for a separate damper. A notable example of damping by dry friction is the Lenoir damper (see figure 2.16), which is commonly coupled with coil springs [14]. The damping effect of this component is proportional to the vehicle mass and is used, for example, in Y25 bogie [19].

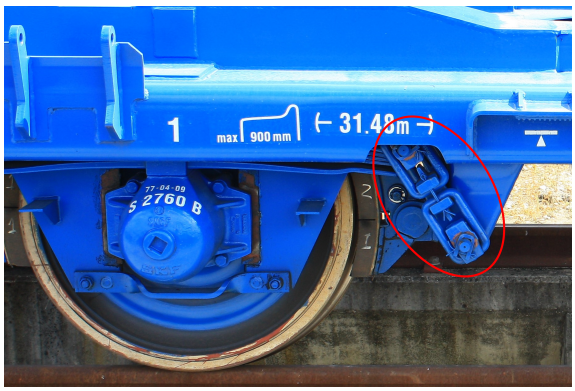

Figure 2.16: Lenoir link.

The specific design of the suspension system may vary depending on the type of freight wagon and the intended cargo. An efficient suspension system is crucial for maintaining a balanced and secure performance, ensuring the safety of both the load and the railway infrastructure. Regular maintenance and inspections are essential to preserve functionality and prolong the operational life of the suspension system.

2.1.6 Brake system

The automatic pneumatic brake system is the most widely used for unpowered railway vehicles globally. In this system, the brake control signals are transmitted from the locomotive to each wagon in the train by altering the pressure in the pneumatic train line brake pipe. Each railway vehicle is equipped with various components for braking, including the brake pipe, air distributor, spare tank, brake cylinder, brake rigging, brake shoes, and an empty-load device [6]. In figure 2.17, a braking system scheme is presented.

The brake system operates by adjusting the air pressure in the train line brake pipe during different modes. The air distributor charges the spare tank and connects the brake cylinder with the atmosphere when the pressure increases. In brake application mode, the pressure decreases, connecting the spare tank with the brake cylinder. The resulting brake force is transmitted to the brake shoes or brake pads, effectively decelerating the vehicle through friction with the wheel treads or brake discs, depending on the brake type [6].

The wheel-rail traction force is directly influenced by the specific axle load of the vehicle, which holds particular importance for wagons, as its empty weight can be up to five times lower than when it is loaded. Therefore, to avoid skidding, the maximum force applied must be adjusted to the vehicle's weight. To achieve this, specialised empty-load devices effectively control the brake cylinder pressure, adapting to the suspension deflection [6].

Because the braking mechanism is controlled by air pressure, there are delays in response proportionate to the distance of each wagon to the locomotive, which impacts the longitudinal train dynamics [6, 14].

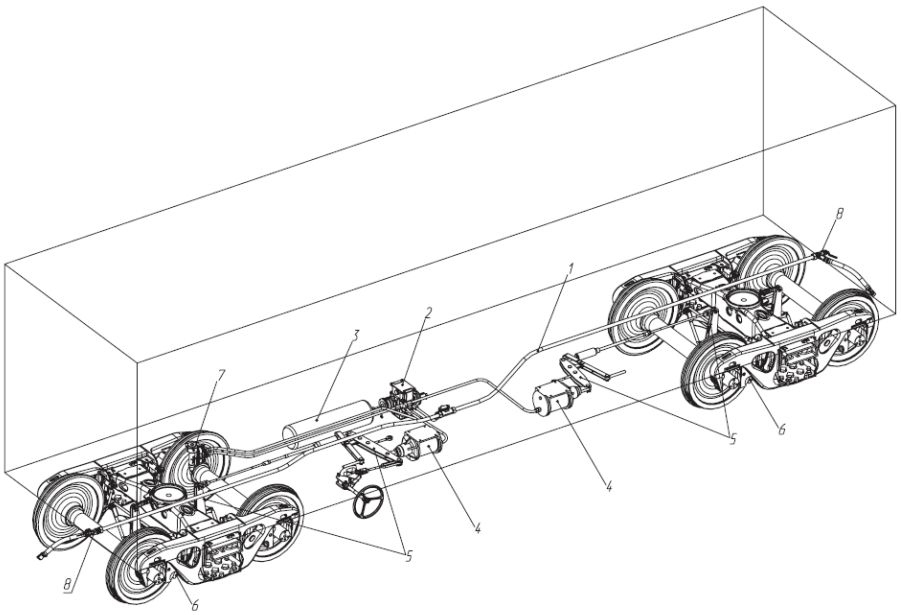

Figure 2.17: General composition of braking equipment on a freight wagon. (1) train line brake pipe; (2) air distributor; (3) spare tank; (4) brake cylinder; (5) brake rigging; (6) brake shoes; (7) empty-load device; and (8) end cock [6].

2.1.7 Coupling

The coupling system is located at the end section of the wagon. This mechanism guarantees a safe and secure connection between individual wagons and the locomotive, ensuring synchronised movement as a single unit. This system enables the efficient transfer of power, braking forces, and control signals from the locomotive to the wagons, facilitating smooth operation and control of the entire train. In other words, it transmits longitudinal tension and compression forces, provides damping of the longitudinal oscillations, and enables the relative movements between vehicles, such as rotation and lateral and vertical displacement, due to the track's configuration. The different wear of the wheels and deflection of the suspension system can also influence the vertical displacement [6, 14].

Several types of coupling systems have been developed and utilised throughout the history of railway transportation. These can be divided into two groups: manual, for example screw coupling (see figure 2.18); and automatic coupling (see figure 2.19).

The first one is the oldest type of coupling and, therefore, less technological. A railway worker connects the two vehicles by hooking one onto another and then tightening the large threaded screw. This system is still broadly used in European freight trains. The damping characteristics

of this connection are ensured by buffers on either side of the screw coupling, which work only in compression. This system is simpler than other automatic ones, thus is cheaper to install [6].

As for automatic coupling systems, the operation is done by running the vehicles against each other. The unique design of the mechanism allows the auto-lock. However, the reverse process, unlocking, has to be done manually. The damping device, draft gear, is located on the central arm of the coupling mechanism itself. Unlike the buffers, it works both in tension and compression. They present a set of advantages compared to manual ones: withstand higher tension and compression forces, allowing an increase in train weight and length; higher speeds when prepping the train for departure and higher safety for railway workers in charge of the coupling [6].

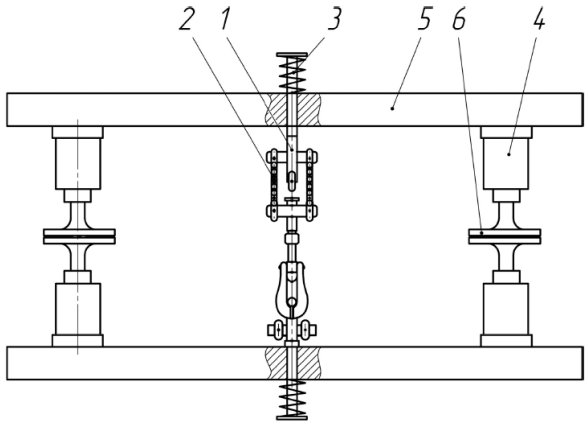

Figure 2.18: Screw coupling scheme: (1) hook; (2) turnbuckle; (3) shock absorber; (4) buffer; (5) end beam of the car body; and (6) buffer plate [6].

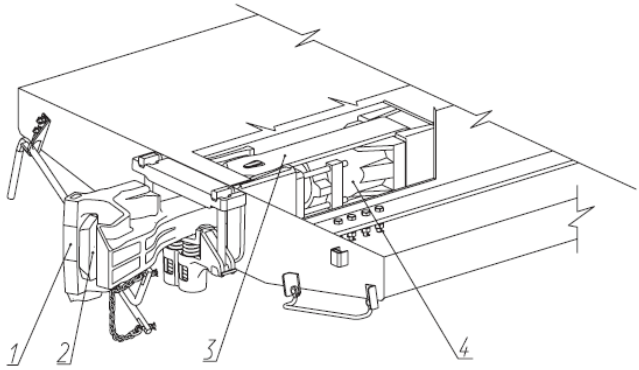

Figure 2.19: Automatic coupler and draft gear: (1) coupler body; (2) lock; (3) yoke; and (4) draft gear [6].

2.1.8 Inner Coupling

When dealing with articulated wagons, the permanent centre coupling is a pivotal aspect to be studied. One well-established method for achieving this connection is the Talbot Type Articulation [21]. It was designed by a German company, *Waggonfabrik Talbot*, and its widespread application is observed in Europe, particularly in the domain of container transport [22].

A significant advantage inherent to this articulation lies in its capacity to decrease wagon weight by eliminating one of the bogies. Instead of featuring two separate wagons, each equipped with two bogies, the system enables the presence of a single wagon, equivalent to the two combined wagons,

yet furnished with only three bogies. Nonetheless, this modification does reduce the maximum transported load the wagon can bear and convey. However, considering the intermodal aspect of container transport, their weight is generally governed by the maximal carrying limit of road vehicles. In sum, the overall efficiency of the wagon is achieved [22].

This coupling mechanism comprises a central pivot that facilitates the rotation of one underframe relative to another, as well as between these underframes and the bogie. Additionally, it features lateral guiding surfaces that ensure precise wagon alignment. Enabling this relative movement between the structures enhances the wagon's curving performance. Essentially, the wagon's length is less constrained by its curving capability, leading to decreased lateral forces contributing to improved wagon stability.

It should be noted that this type of articulation encounters more intricate load scenarios than the coupling mechanisms delineated above. Firstly, it experiences both tension and compression forces—whereas, in other systems, these loads are borne by distinct components of the linkage (the buffers are compression actuated, and the coupling is tension actuated). Secondly, it is responsible for transferring vertical forces to the bogie [22].

Thus, the structural criteria that this mechanism has to fulfil are stipulated as follows: "The longitudinal strength of the inner coupling(s) shall be equal or higher than the one of the end coupling(s) of the unit" as outlined in section 4.2.2.1.2 of the WAG-TSI [23]. In essence, this implies that the requirements, spanning static and fatigue considerations, applicable to the several constituents that compose the coupling system must be met.

Furthermore, the overall main dimensions of the Talbot Coupling are detailed in Annex L of EN 16235:2013 [21]. These dimensions can be visualised in figures 2.20 and a real example of this coupling mechanism is shown in figure 2.21.

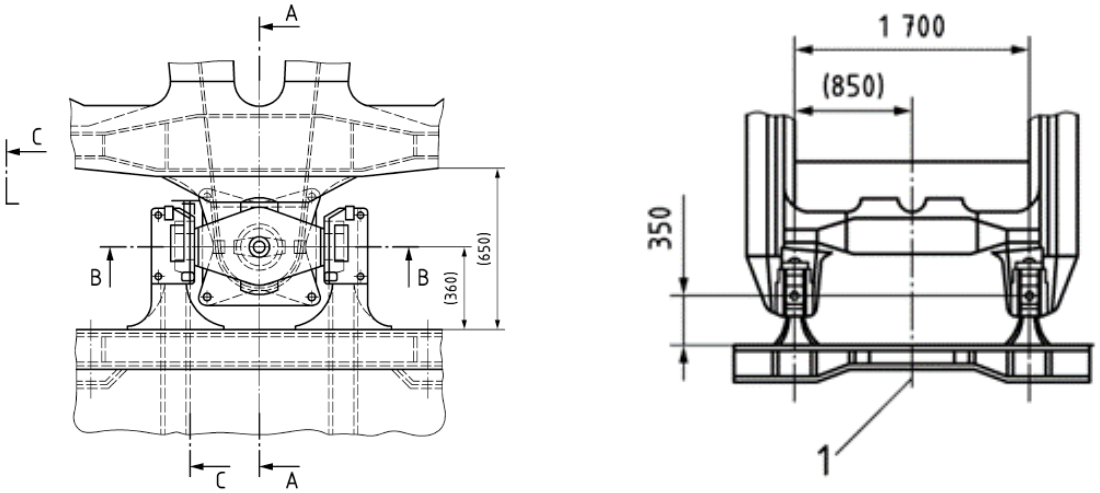

Figure 2.20: Talbot Type Articulation dimensions [21].

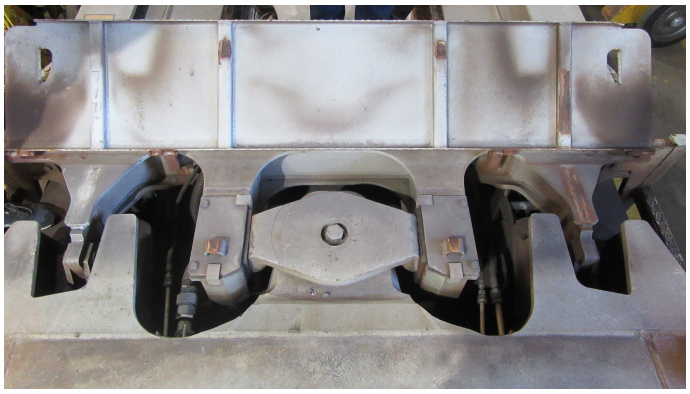

Figure 2.21: Talbot articulation in the Sggrss wagon.

2.2 Design of freight wagons

The advancement of computational methods has significantly enhanced the design and analysis of railway wagons, with the Finite Element Method (FEM) emerging as a potent tool. This technique enables the simulation and anticipation of a wagon's static, dynamic, and fatigue structural behaviour, accommodating a wide range of load cases and operational conditions.

This procedure offers advantages, such as reducing time and costs associated with iterative design processes before creating physical prototypes for experimental testing [24, 25]. This approach allows for structural optimization by analyzing stress distribution. For instance, it becomes possible to minimize thicknesses and adapt cross-sectional areas in regions with low stress, resulting in weight reduction and increased payload capacity, ultimately boosting the vehicle's profitability [26]. This approach has various successful applications, such as in the Sustrail project [27], where a 60ft flat wagon was optimized by adopting high-strength steel and changes in beam profiles. Numerical simulations played a pivotal role in studying stress distribution, culminating in a notable 20-25% reduction in weight with the proposed design modifications.

Additionally, new materials, design elements, technologies, and different wagon solutions can be introduced by employing this methodology. It is also used in retrofitting older models [28].

For instance, M. Płaczek et al., in 2015 [28], explored the integration of composite panels into box car sidewalls to reduce the thickness of the steel walls and subsequent wagon weight. Meanwhile, authors W. Krason et al., in 2014 [29], pursued a solution for simplified loading and unloading of wagons for intermodal transport of class U, without the need for significant infrastructure changes. Their innovative wagon's non-standard layout necessitated an altered design process approach, where numerical simulations became integral. This iterative approach simulated each substantial design modification to precisely forecast its impact on the entire wagon structure.

The research conducted by P. Šťastniak et al., in 2018 [30], aimed to develop a new freight wagon tailored for container transport, while also investigating its structural behaviour through simulations. They state that the final result is a wagon design that offers increased capacity and heightened resource efficiency compared to prevailing intermodal transport wagons. The initial segment of the study is dedicated to determining the optimal wagon length. The study ultimately establishes that an 80ft wagon configuration is the most advantageous choice, enabling optimal utilization of available loading space. This configuration facilitates the transportation of an equivalent or even greater number of containers with fewer axles and reduced deadweight. Additionally, the 80ft wagon exhibits aerodynamic benefits due to the closer container arrangement and noise

reduction due to the lower number of axles per wagon.

Reviewing existing articles has played a pivotal role in comprehending the methodologies employed in structural analyses of freight wagons, focusing on those designed for container transportation. It helped to gain knowledge on the load cases to be applied, the standards that the structure needed to comply with, and how the boundary conditions on the model are applied.

In the context of meshing the model, S. Slavchev et al., in 2015 [31], researched whether shell or solids elements were more accurate for the model. Their investigation did not yield definitive conclusions, and in the end, the authors suggest the use of hybrid models, incorporating both shell and solid elements for a more accurate representation.

2.3 Regulatory Environment

The European rail freight sector has undergone a significant transformation over the years. In 1990, the industry was fragmented, with each member state having its own set of regulations and standards. However, this landscape has evolved into a more unified and efficient system that enables seamless cross-border rail travel.

The primary objective of this transformation was to enhance the competitiveness of railways and regain market share that had been lost to road transport. This transition was greatly facilitated by the directives introduced by the European Commission in 2001. These directives provided a framework for harmonizing railway standards and regulations across European countries.

Furthermore, the establishment of the European Railway Agency (ERA) played a crucial role in this process. ERA oversees various Technical Standards for Interoperability (TSI) that define standardized requirements across the railway sector. Among these TSIs, the WAG-TSI [23] specifically pertains to freight wagons, addressing important aspects related to their design and interoperability within the European rail network.

This shift towards standardization and interoperability has not only streamlined rail freight operations but has also contributed to the overall efficiency and competitiveness of the European rail industry.

The UIC, International Union of Railways, is a member organization with the primary objectives of promoting interoperability and creating new global standards for railways. To achieve these goals, the UIC publishes a series of technical standards and guidelines known as "leaflets." These leaflets provide guidance and set standards for railway systems worldwide, and are often used as guidelines for the European Standards.

In the context of structural analysis for freight wagons, there is a European standard of great relevance, EN 12663, specifically Part 2 [32], which defines the structural requirements of railway vehicle bodies. It establishes detailed guidelines for the structural requirements of these wagons, including load requirements, procedures for experimental testing, and even a validation program to ensure that wagons meet the necessary safety and performance standards.

This validation program depends on the level of innovation in the design and the extent of changes in its application, which includes factors such as usage intensity and years in service. The table 2.2 provides a summary of this validation program. In essence, new designs must undergo the tests specified in this standard, while models based on existing designs require fewer tests for validation.

Table 2.2: Summary of validation programme [32].

	Complete structural analysis	**Local or global comparative structural analysis**	**Tests specified in this standard**	**Fatigue and/or service tests**
New design	N/A	N/A	yes	only required if tests specified in this standard do not show sufficient fatigue strength
Evolved design and/or new application Identical design and new application	no	yes	no or reduced test programme	only required if other methods do not show sufficient fatigue strength
Evolved design, similar application	no	yes	no or reduced test programme	no

NOTE: A new design is a product (vehicle or component part) that is newly created and has no direct connection with any existing similar product. An evolved design is a product (vehicle or component part) that is based on an existing similar product and has direct connection with that existing product.

This standard outlines the requirements for the wagon body. However, other components and mechanisms are standardized by separate documents. A few pertinent examples include:

1. Draw Gear and Screw Coupling - Regulated by EN 15566 [33];
2. Automatic coupler - Regulated by EN 16019 [34];
3. Buffers - Regulated by EN 15551 [35].

Standards also extend their reach into the realm of manufacturing. An illustrative example can be found in wagon construction, where welding requirements are rigorously stipulated by EN 15085 [36]. This standard is a pivotal cornerstone, ensuring the integrity and quality of welding processes, which are paramount in these vehicles' fabrication.

A new standard, prEN 17149 [37], is currently being developed to outline the strength assessment of railway vehicle structures. This standard is divided into several parts, each addressing specific aspects:

- Part 1: General
- Part 2: Static strength assessment
- Part 3: Fatigue strength assessment based on cumulative damage

This forthcoming standard is expected to bring substantial benefits by providing a refined and comprehensive framework for structural evaluations. Its meticulous approach to fatigue assessment, in particular, offers valuable insights and procedures, filling a gap that existed in previous standards. As a result, this standard will empower engineers to conduct more precise and thorough analyses, thereby enhancing the overall quality and safety of railway wagons.

The world of railway standards is vast and intricate, covering an extensive array of intricate details and components. These standards span across a multitude of categories, from structural requirements and safety protocols to manufacturing processes and material specifications. The sheer volume and diversity of these standards reflect the comprehensive nature of the railway industry, where precision, safety, and interoperability are paramount. Each standard plays a vital role in ensuring the seamless functioning of this complex transportation network.

Chapter 3

Case Study - Sggrss Wagon

This chapter is dedicated to the presentation of the project's case study, the Sggrss wagon. It provides a detailed description of the geometric model, followed by an elucidation of the characteristics of the FEM model. Essential details such as meshing, applied boundary conditions, and the various load cases considered in the analysis are thoroughly explained in this section.

3.1 Introduction of case study

Embedded within the broader scope of the Smart Wagons project, which entails the construction of a freight wagon for container transport, this Thesis aims to craft a preliminary model of the wagon's underframe and subsequently conduct a structural analysis.

It is important to note that the current model focuses exclusively on the wagon's underframe, the key element slated for construction. Distinct components like the bogies, the braking system and others are procured independently. Presently, their integration into the structure is not accounted for. However, it is pertinent to acknowledge that future analyses must incorporate them into the underframe design.

The wagon under development belongs to the Sggrss classification—a special flat wagon with bogies (S) for accommodating containers up to 80 ft (gg), featuring an articulation (r) and possessing a maximum speed capability of 120 km/h (ss). An example of this type of wagon, produced by *Greenbrier*, can be seen in figure 3.1.

Some UIC leaflets host certified technical drawings of certain wagon models, regrettably, the sought-after specifications for this particular model proved elusive. This preliminary geometry proposal was the outcome of a comprehensive analysis that explored several existing wagon solutions available in the market. Through a rigorous examination of various design options and careful consideration of industry standards, this proposed geometry was developed as an informed and well-researched choice.

Finally, the numerical analysis is performed using ANSYS software, the ANSYS Mechanical APDL.

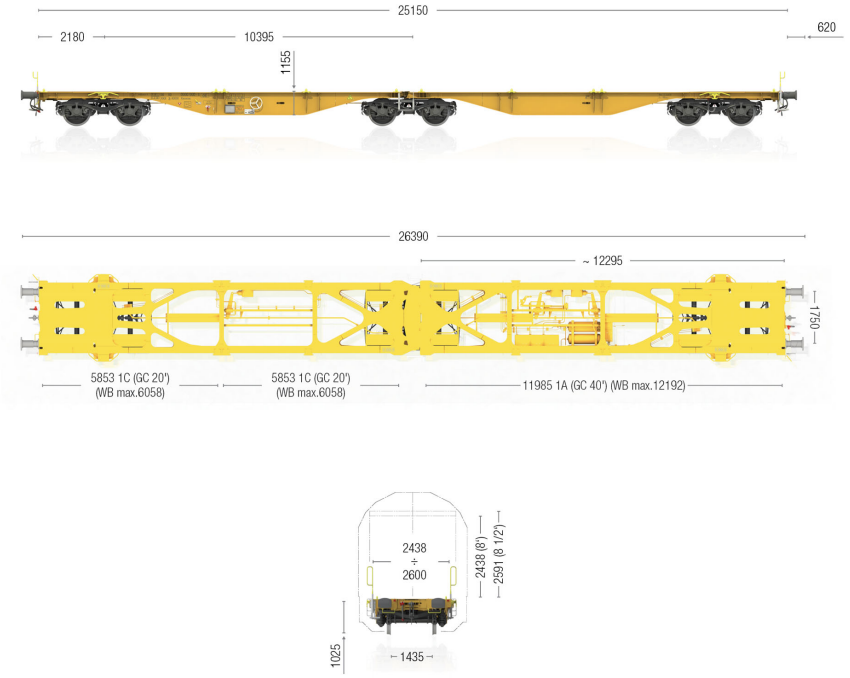

Figure 3.1: Example of Sggrss wagon [38].

3.2 Geometrical Model

The underframe of the wagon comprises two prominent side girders that run longitudinally along its length. These girders are interconnected by transverse beams strategically positioned to distribute loads and enhance structural integrity. The collaboration between the side girders and transverse beams forms a robust frame that supports the wagon's cargo and ensures its stability during railway operations. The complete wagon features two symmetrical frames connected by a Talbot coupling system, hence, only half of the wagon is modelled (see figure 3.2). The structure is symmetric about the x-axis and was primarily divided into two key components: the main longitudinal girder and the various transverse beams. Some overall wagon dimensions are as follows:

- Distance between bogies: 10 m;
- Total length (without central articulation): 12 m;
- Width: 2.3 m.

The girder (see figure 3.3) is shaped similarly to an I-beam with a bottom and top flange and web, and exhibits varying cross-sectional dimensions along the wagon's length. Due to this variability, meticulous attention was dedicated to this component. The girder is composed of distinct welded plates meticulously assembled to achieve the desired profile. Different sections encompass changes in both the geometry and thickness of the web and flanges. The top flange showcases thickness variations ranging from 18 to 25 mm, with the highest thickness concentrated near the central articulation. The web thickness ranges from 8 to 12 mm, with 8 mm employed at the central region of the girder—corresponding to the web's higher section. The bottom flange exhibits the most substantial thickness contrast, spanning from 16 to 30 mm. In summary, aligning with what is stated above, the regions with the minimal thickness are primarily situated in the centre

of the wagon, whereas the thickest portions are concentrated around the bogie positions. Notably, these areas coincide with the girder's minimal web height. Another noteworthy characteristic of this beam is its off-centre web and the changing alignment and geometry of both the flanges and the web along its length. Additionally, there is a distinct section where the girder transitions from an I-beam to a box-beam configuration (detail 1 in figure 3.3). This diversity in geometry and thickness can be attributed to a topology optimization undergone during the wagon's design to enhance weight efficiency.

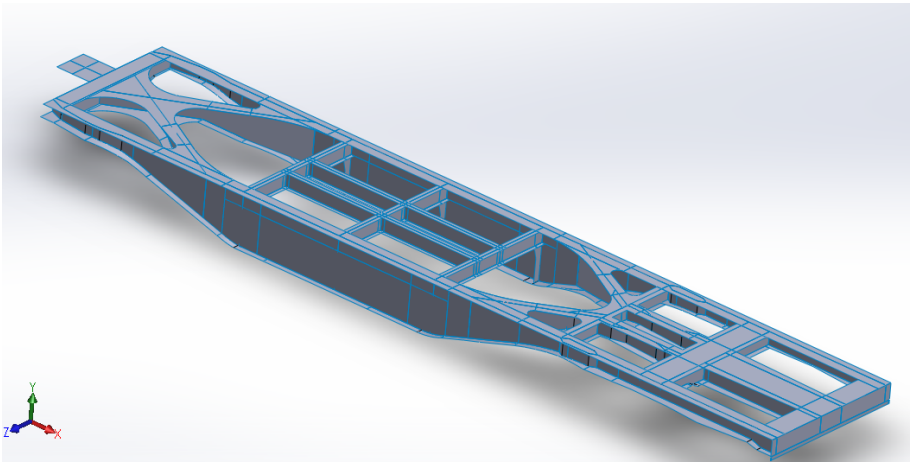

Figure 3.2: Geometrical model (Solidworks Software).

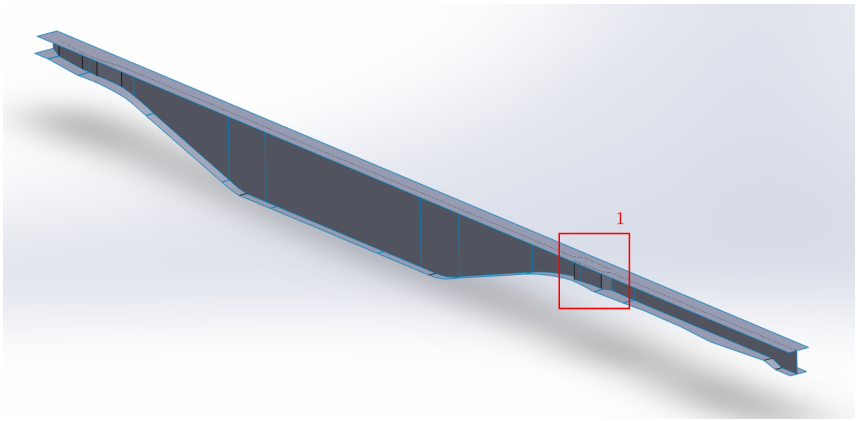

Figure 3.3: Geometrical model: girder (Solidworks Software).

Subsequently, the transverse beams were constructed, focusing on aligning their dimensions within the model. Initially, the approach involved creating the upper plates and placing the corresponding webs. Throughout this process, there were instances where assumptions had to be made about some dimensions due to measurements uncertainties and obscured areas. A notable example is the transverse beam where the bogie is connected—a critical junction in the wagon's structure. This area features a box-beam configuration, making it impossible to ascertain details like the thickness of the webs and the internal reinforcement structures within it. This information gap is particularly crucial, given that this region serves as a pivotal point for the wagon, where the transfer of vertical loads occurs. This area is highlighted in the figure 3.4 as number 1.

In the middle section of the wagon, there are five standardised IPE 220 beams (detail 2 in figure 3.4). Modelling the other transverse beams posed certain challenges due to the inclination of the lower flange and the presence of rounded sections. Due to insufficient information, the wagon's end section suffered significant simplifications. In future iterations, this structure would require more

detailed modelling to ensure it accommodates and withstands the requirements imposed by the buffers and coupling mechanism. The wagon incorporated stiffeners to enhance structural rigidity. In this model, it is included three stiffeners on each side, aligned with the central I-beams (see figure 3.5).

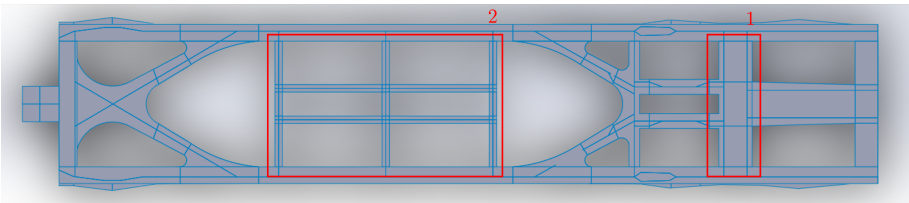

Figure 3.4: Geometrical model: transverse beams (Solidworks Software).

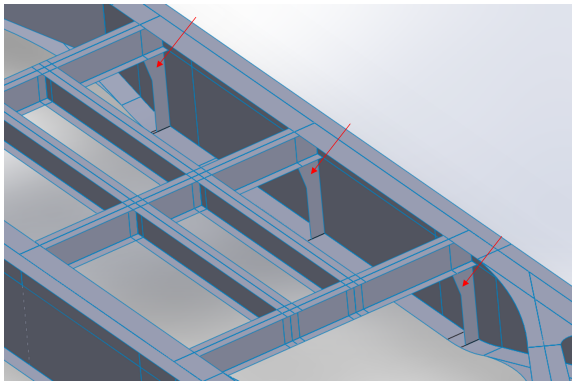

Figure 3.5: Geometrical model: stiffeners (Solidworks Software).

Furthermore, it should be noted that the modelling of the central articulation was beyond the scope of this analysis. Instead, a simplified square area was created as a placeholder for boundary conditions. The dimensions for this square were sourced from the pivot area of the central articulation, as outlined in EN 16235:2013 [21] (see subsection 2.1.8). A substantial thickness (50 mm) was assigned to ensure adequate rigidity of this component in relation to the wagon's structure.

The complexity of the geometry prompted the adoption of CAD software, Solidworks, to streamline the modelling process. The model was crafted as surfaces to align with the intention of the finite element analysis of employing shell elements. Thickness assignments were integrated alongside element allocations.

However, this dual-software approach introduced complications. Importing the CAD model into ANSYS highlighted issues with non-coincident lines among adjacent zones, preventing unified behaviour as mesh elements floated independently. Rectifying this required meticulous reworking of areas to ensure shared elements, proving to be a time-consuming endeavour.

Finally, while some simplifications were made regarding curvature radii and minor details throughout the model, these decisions were driven by their lack of significance for the finite element analysis. Notably, welding was not considered. Instead, the model is a continuous part.

This detailed model, crafted with close alignment to accurate measurements, holds significant importance for this study. Despite the intricate nature of its creation, the accuracy of this model carries substantial value. It acts as a foundational step for the project, offering an accurate reference point for various aspects like manufacturing plans. The comprehensive representation of the real wagon enhances the understanding of the structure and lays a robust base for further study. This

careful approach, despite its challenges, not only highlights the thoroughness of the analysis but also provides a solid foundation for upcoming phases of the project.

3.3 Finite Element Model Description

This section presents a detailed description of the Finite Element Model of the wagon structure. First, it is set the coordinate system for the model and a consistent unit system throughout the structural analysis. Moreover, the most appropriate element type for this analysis is defined, and a mesh convergence study is conducted to ensure accuracy of the results. Finally, the boundary conditions of the model are outlined, as well as the load cases applied.

3.3.1 Coordinate System

The coordinate system is shown in figure 3.6. The positive direction of the x-axis (corresponding to vehicle body longitudinal axis) is in the direction of movement. The positive direction of the y-axis (corresponding to vehicle vertical axis) points upwards. The z-axis (corresponding to vehicle transverse axis) lies in the horizontal plane completing a right hand coordinate system.

3.3.2 Unit system

The unit system is presented in the table 3.1.

Table 3.1: FEM system of units.

Quantity	Mass	Length	Time	Force
Unit	ton	mm	s	N

All other input and output quantities are based on the above mentioned units, i.e., density in ton/mm^3, stress in N/mm^2 (MPa) and acceleration in mm/s^2.

3.3.3 Material

The wagon frame will be constructed from structural steel S355J2 and their properties, according to EN 10025-3 [39], are shown in Table 3.2.

Table 3.2: Material properties of steel S355J2.

Young Modulus [MPa]	**Poisson's ratio**	**Density [kg/m^3]**	**Yield Strength [MPa]**	**Tensile Strength [MPa]**
2.10E+05	0.3	7850	355	470

3.3.4 Mesh

The selected element type for the structural analysis is Shell 181, a four-node element featuring six degrees of freedom at each node, encompassing translations along the x, y, and z axes, as well as rotations about the x, y, and z axes [40]. This element is particularly suited for analysing shell structures with varying thickness, making it applicable to the model's thin to moderately thick sections (ranging from 8 to 30 mm). This choice was informed by a balance between accuracy and computational efficiency, as the shell elements reasonably represent the structural behaviour while minimizing computational demands.

3.3. Finite Element Model Description

This model comprises a total of 7606 elements and 7619 nodes. Predominantly, quadrilateral elements are employed, and a uniform mesh size was set with a size element of 100 mm for the areas. A local mesh refinement was performed in the areas of the bogie pivot boundary condition by setting a size element of 40 mm, with the objective of having a higher number of nodes to support. In figure 3.6, the mesh of the model is presented.

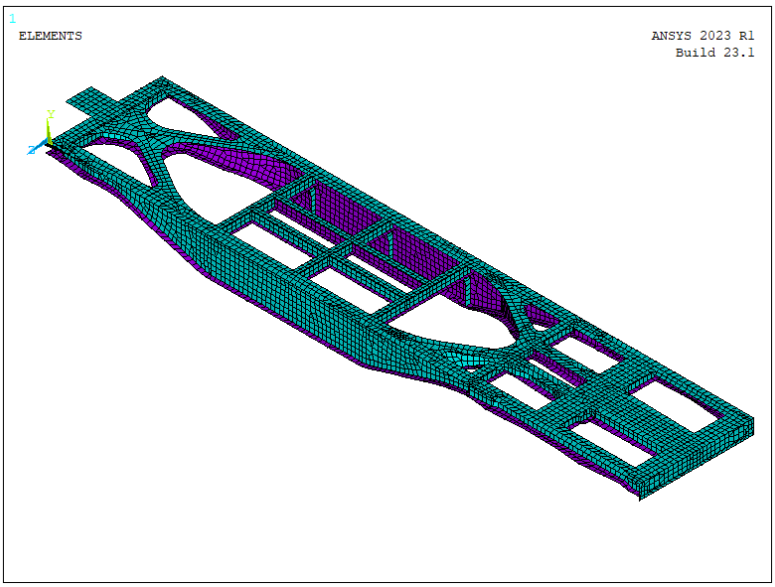

Figure 3.6: Meshed model.

Finally, a mesh convergence analysis is conducted to investigate the impact of mesh size on the results. The convergence of the maximum y displacement for the second vertical load case, VLC2, (please refer to section 3.3.6 for detailed explanation of the load cases) was studied, and the graphic with the results is depicted in Figure 3.7. It is evident that a plateau is observed after reaching 7606 elements, implying that this element count is sufficient to ensure mesh-independent results. Additionally, it is worth noting that this mesh convergence study was carried out using values of displacements, instead of a stresses, as the latter may compromise the accuracy of the results due to singularities and stress concentrations in the model.

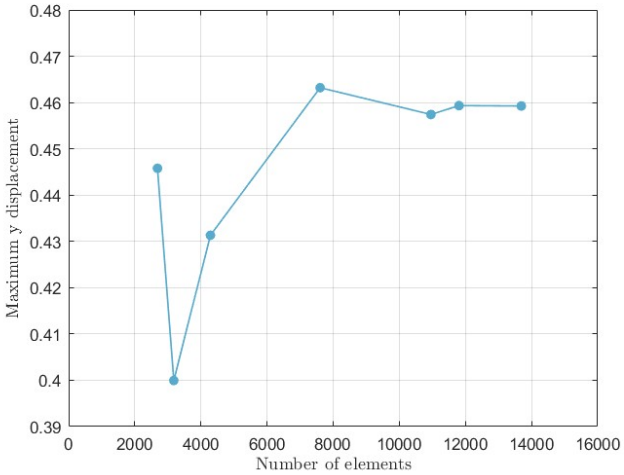

Figure 3.7: Mesh convergence analysis.

3.3.5 Boundary Conditions

The correct implementation of the problem's boundary conditions is a key aspect to obtain reliable results. For this study, the conditions applied correlate with the underframe-bogie connections and the inner coupling mechanism, since only half of the complete wagon structure is simulated.

3.3.5.1 Inner Coupling

The boundary conditions applied at this end of the wagon are in line with the Talbot Type Articulation operation, described above in section 2.1.8. Thus, three vertical supports (Uy=0) were applied on the points where the lateral guiding surfaces would be and on the centre point of the pivot, and a simple support on the transverse axis of the central block (Ux=0). Figure 3.8 shows their application in the model.

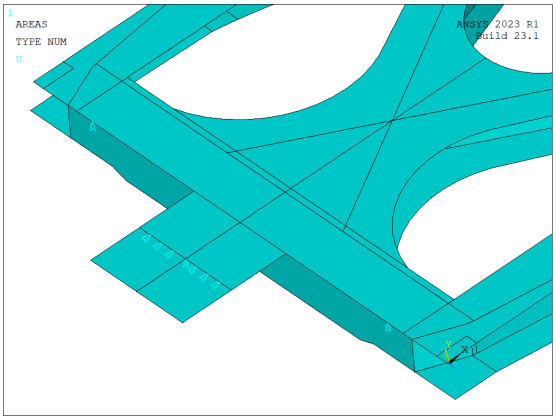

Figure 3.8: Inner coupling boundary conditions.

3.3.5.2 Bogie

The connection between the underframe and the bogie is achieved through the centre pivot top, a flat plate with a bowl-shaped indentation at its centre that tightly fits onto the centre bowl of the bogie, creating a stable connection and allowing controlled rotation and articulation between these two elements. It is secured to the wagon structure using bolts or fasteners, ensuring effective load transfer between the components. In figure 3.9, it is possible to observe the connection between the bogie and the body of the wagon and in figure 3.10, the bogie pivot and the pivot top are presented in more detail.

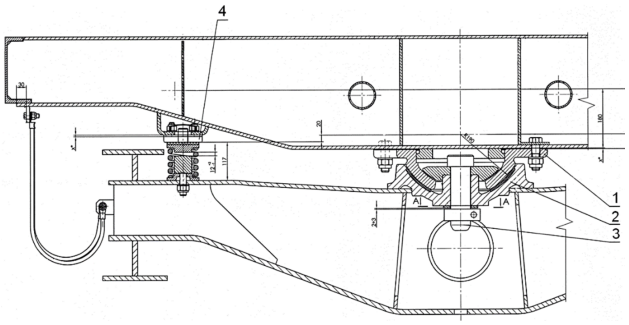

Figure 3.9: Connection between the body and bogie frame. 1 - pivot top, 2 - centre bowl, 3 - pivot pin, 4 - side bearer [41].

3.3. Finite Element Model Description

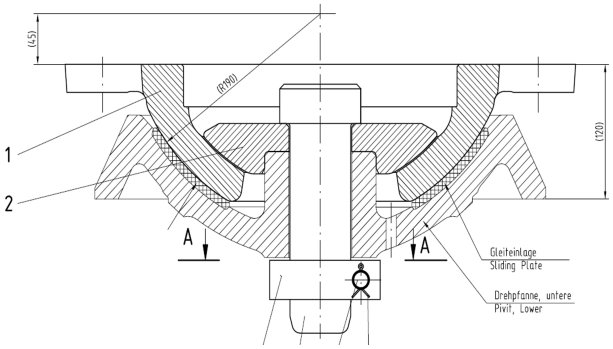

(a) Technical drawing of the bogie pivot. 1 - pivot top.

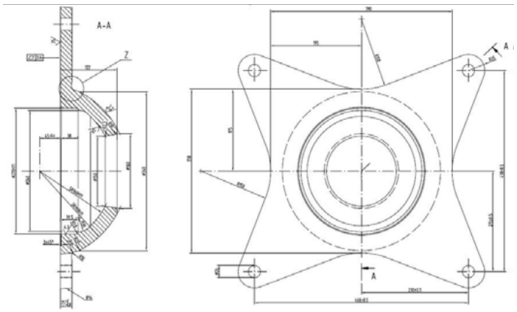

(b) Technical drawing of pivot top.

(c) Pivot top picture.

Figure 3.10: Bogie pivot (adapted from [17]).

This boundary condition can be replicated by supporting the area of the wagon that comes into contact with this component. However, due to the lack of information regarding this connection in the studied wagon and the accurate dimensions of this component, it was deemed sufficient to support an approximate area in the model. In essence, all nodes within this designated area are prevented from having vertical displacement (Uy=0), as can be seen in figure 3.11.

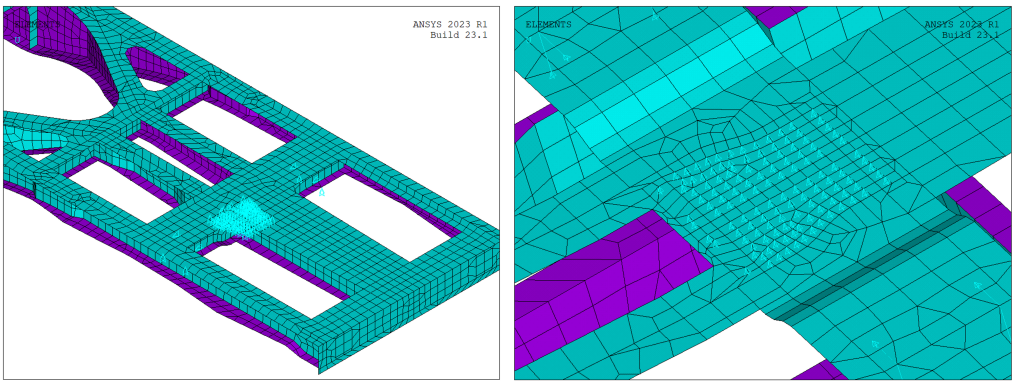

Figure 3.11: Bogie pivot boundary conditions.

Additionally, the bogie is equipped with side bearer springs to enhance the wagon's stability. These differ from traditional suspension elements as they focus on maintaining the wagon's equilibrium. Under optimal conditions of linear movement, where the load distribution is perfectly balanced, the involvement of these components becomes unnecessary. However, when navigating through a curve, these springs are actuated (based on the direction of the curve) [17]. They are

designed to counter lateral displacements, and by accounting for these lateral effects, the finite element model more faithfully mirrors the real-world behaviour of the wagon's underframe-bogie connection. Their placement is shown in figure 3.9, and a more detailed drawing is presented below in figure 3.12.

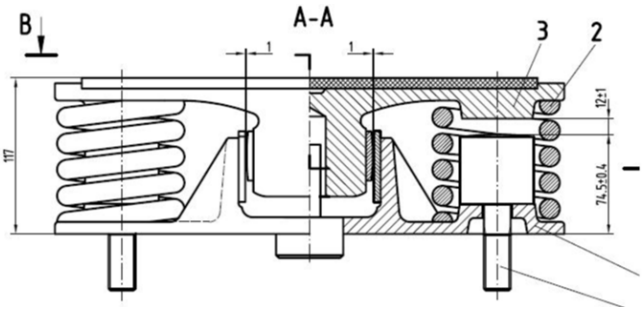

Figure 3.12: Side bearer spring drawing [17].

This boundary condition was accomplished by introducing a spring element on the location of these components. These were implemented using the COMBIN14 element type in ANSYS, where each spring has longitudinal stiffness of 285 N/mm and a length of 119 mm, following what is stipulated in annex H.2 of EN 16235 [21]. Moreover, a transversal spring (in z-direction) was added with the same length but with a thousand times greater stiffness (k=285000 N/mm). This was done to simulate a much higher stiffness in this direction. Note that the free ends of the spring elements are fixed in the direction they are defined. In figure 3.13, the springs' implementation in the model is presented.

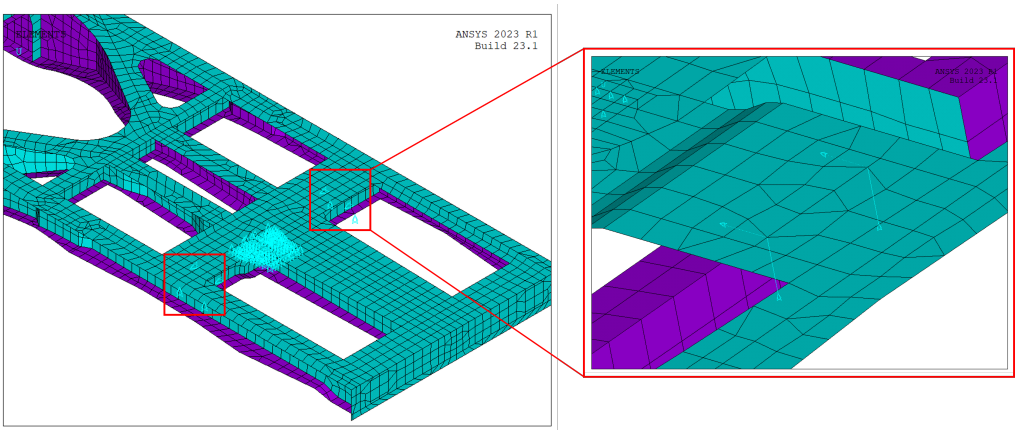

Figure 3.13: Side bearer springs boundary condition.

In the future, there is potential to enhance the representation of boundary conditions in the model. Currently, the boundary conditions at the bogie primarily consist of vertical supports in the pivot area. However, a more refined approach could involve replacing these vertical supports with a multipoint constraint system. Considering a single node to represent the pivot would allow for an accurate simulation of its rotations. This approach would align the model more closely with real-world conditions, providing a more accurate depiction of the wagon's behaviour.

3.3.6 Load Cases

To assess stresses and deflections, each new wagon is subjected to numerical and experimental studies in compliance with international standards. The loading conditions to be applied are described in European standard EN 12663-2:2010 [32], Leaflet 577 [42] of the International Union of Railways (UIC) and some other documents.

According to these, several load cases are established. Among them, the ones applied in this study can be divided into three groups: longitudinal static loads (HLC), vertical static loads (VLC) and superposition of static loads (SLC). They can be consulted in table 3.3 and are explained in more detail below. Note that all horizontal load cases are to be applied in combination with the structure self weight, achieved by adding an acceleration in the vertical axis of 9.81 m/s^2. Moreover, m_1 and m_3, as referenced in the table, correspond to the design mass of the vehicle body in working order (excluding bogies) and the standard design payload, respectively. Detailed definitions for both will be provided in the description of the vertical load cases.

Table 3.3: Load Cases.

Load Case	**Description**
HLC1	Compressive force at buffer axis height of 2000 kN (table 2 of [32])
HLC2	Tensile force in coupler area of 1500 kN (table 5 of [32])
VLC1	Vertical load from weight of 40 ft. container (table 6 of [32])
VLC2	Vertical load from weight of 2×20 ft. containers (table 6 of [32])
SLC 1	HLC1 + $g \times (m_1 + m_3)$ (2×20 ft. containers) (table 9 of [32])
SLC 2	HLC2 + $g \times (m_1 + m_3)$ (2×20 ft. containers) (table 9 of [32])

Longitudinal static loads:

1. HLC1

   This load scenario involves applying a compressive force of 2000 kN at the axis height of the buffers. In other words, a symmetric concentrated load must be applied to each buffer. However, in this project and following the approach outlined in [43], this force is distributed over an area equivalent to the buffer's base. Effectively, the load applied to the buffer is transmitted through its various parts, subsequently being distributed uniformly to the front beam of the underframe. Using a distributed load instead of a concentrated one offers a more accurate representation of real-world forces, minimising stress concentration at the point of application. In figure 3.14a, the application of this load case can be seen.

2. HLC2

   The standard outlines the process of applying a tensile load to the draw gear stops. However, in this model, the linkage between the underframe and the draw gear is not portrayed. To simulate this, the maximum load of 1500 kN was distributed across four points on the front beam. These points were strategically chosen to align with the positions of the draw gear stops, effectively replicating the intended scenario. This can be observed in figure 3.14b.

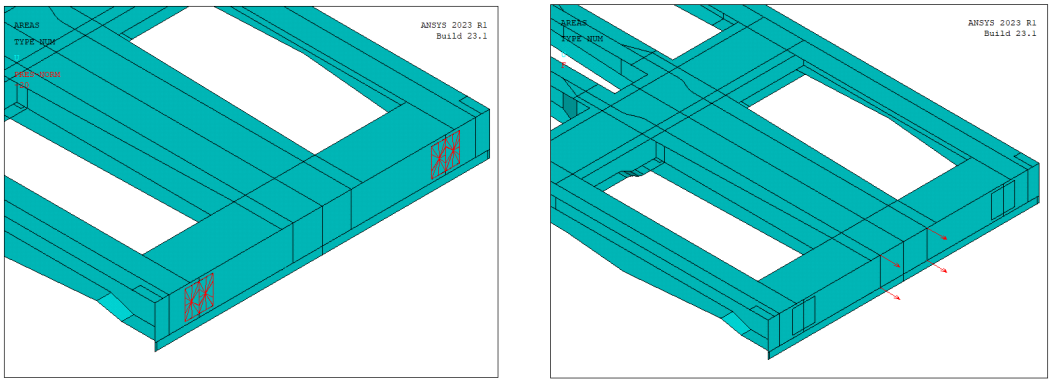

(a) HLC1 **(b)** HLC2

Figure 3.14: Application of longitudinal static loads.

Vertical static loads:

Concerning vertical load scenarios, the analysis exclusively encompasses the maximum operating load. This load accounts for the wagon body's and cargo's combined weight, determined through Equation 3.3.1 [32].

$$F = 1.3 \times g \times (m_1 + m_3) \tag{3.3.1}$$

Where,

- m_1 is the design mass of the vehicle body in working order (without bogies);
- m_3 is the normal design payload.

The following equation 3.3.2 provides the value of m_3 with respect to the maximum allowed load per axle, which is 22.5 ton.

$$m_3 = 6 \times 22.5 - m_1 - 3 \times m_2 \tag{3.3.2}$$

The load per axle is multiplied by six to account for the six axles, considering the wagon's configuration with three bogies, each having two axles. The selected bogie for this project falls within the Y25 category. With a mass denoted as m_2, each bogie weighs 4300 kg and is sourced from an established Sggrss wagon catalogue provided by *Talleres Alegría* [44]. The wagon frame's mass, m_1, was obtained from the FEM model, totalling 10.812 tons. It is important to note that this value underestimates the complete wagon weight as it excludes the centre articulation, attachments, coupling, and braking system. Nonetheless, this approach ensures a more cautious analysis, contributing to a conservative assessment.

The total force is divided into two parts: one associated with the underframe's mass, m_1, and the other with m_3, representing the standard design payload. For the first component, the load is generated by introducing the acceleration of gravity into the model, amplified by a factor of 1.3. The second component is applied as a concentrated force on the connection points between the wagon frame and the container, also multiplied by a safety factor of 1.3. Each container is supported by four spigots positioned at its corners. These spigots play a crucial role in restricting container movement in relation to the wagon. The positioning of these spigots adheres to standardized guidelines outlined in UIC Leaflet 571 [45], and additional visual reference can be found in Figure 3.15.

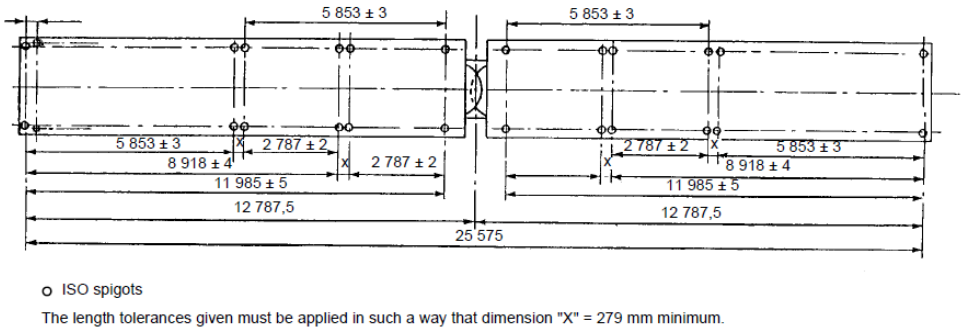

Figure 3.15: Spigot positioning for 80 ft wagon [45].

This approach enables the consideration of various load scenarios aligned with diverse container transport combinations. This wagon can carry different sizes of standardised containers, ranging from 20 ft to 40 ft. Their positioning can be easily observed in the scheme presented in figure 3.16. For the scope of this study, the focus centres on the transport of either a single 40 ft container, VLC1, or the transportation of two 20 ft containers, VLC2. The concentrated force associated with each loading configuration is documented in Table 3.4, while the specific application of these forces is visually illustrated in Figure 3.17.

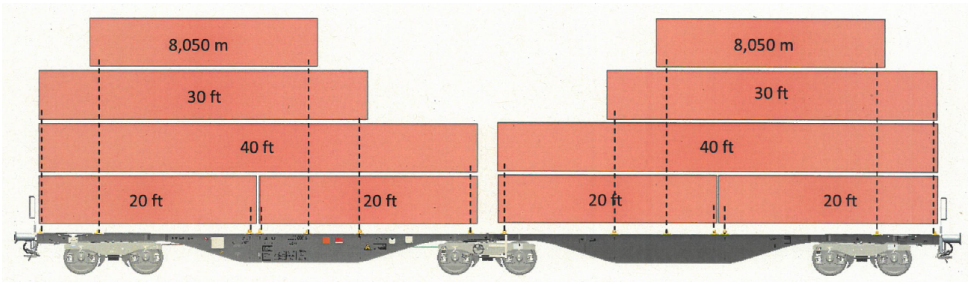

Figure 3.16: Cargo options [44].

Table 3.4: Concentrated force value for VLC1 and VLC2.

Load Case	Force
VLC1	177 406.6 N
VLC2	88 703 N

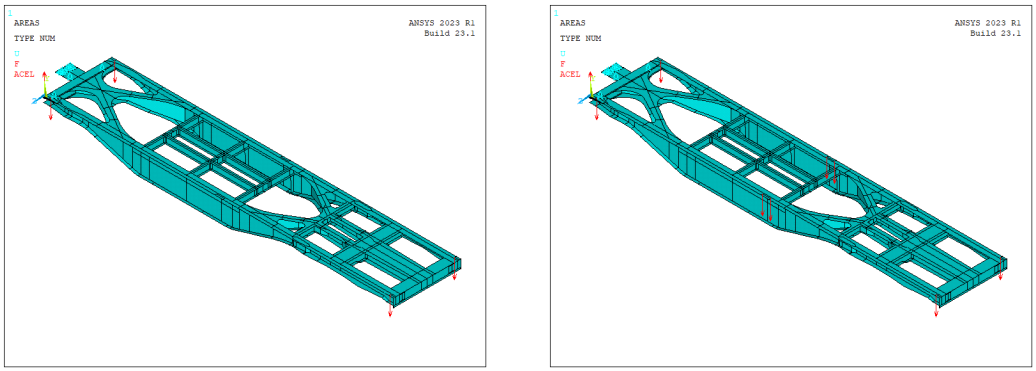

(a) VLC1 **(b)** VLC2

Figure 3.17: Application of vertical static loads.

Superposition of static loads:

In order to demonstrate a satisfactory static strength, the standard proposes that the superposition of static load cases should be considered. Within this framework, two primary cases are proposed. The first, denoted as SLC1, emerges from the combination of a compressive force applied at the buffer axis height (HLC1) and the vertical load stemming from the cumulative wagon weight and maximum cargo (i.e., $g \times (m_1 + m_3)$). The second case, SLC2, mirrors the same vertical load conditions as SLC1, incorporating a tensile force within the coupler area (HLC2). The distribution of vertical forces is the same as in VLC2, i.e. two 20 ft containers.

Furthermore, it is possible to take into account the load distribution of the 40 ft container. Nevertheless, the selected load case is anticipated to be more demanding due to the placement of loads at the girder's midpoint, as opposed to solely at the extremities, where the loads are more directly transferred to the bogies, i.e. the boundary condition.

Chapter 4

Structural Analysis

This chapter is dedicated to analysing the results obtained from the finite element simulations. It encompasses a static and fatigue analysis, each with its respective methodology description. Subsequently, a comprehensive discussion of the results is presented, followed by an assessment of their compliance with the established structural requirements. Finally, a modal analysis is performed to evaluate the natural modes of vibration, providing valuable insights into the structure's dynamic behaviour. This preliminary modal analysis is important for planning future dynamic and instability studies, enhancing the knowledge of the wagon's response to various dynamic loads and potential resonance scenarios.

4.1 Static Analysis

4.1.1 Methodology

To establish the structure's static strength and structural stability, a set of criteria must be met, encompassing strength and deformation considerations.

According to EN 12663-1 [46], calculation and/or testing must demonstrate that no significant permanent deformation or fracture of the structure as a whole, any individual element, or any equipment attachments will occur under the prescribed design load cases. The requirement must be satisfied by meeting the yield or proof strength presented in equation 4.1.1.

$$U_1 = \frac{\sigma_c S_1}{R} \leq 1 \tag{4.1.1}$$

Where,

- U is the utilisation;
- R is the material yield stress (see table 3.2);
- σ_c is the calculated stress;
- S_1 is the safety factor.

When the design is verified only by calculations, the safety factor is 1.15. However, when experimental tests are also performed, and the results of both approaches are very similar, S_1 can be considered 1. In this case, the value of 1.15 is employed.

The standard also defines that in the case of ductile materials, it is not necessary to fulfil the above criterion in areas of local stress concentration, and it is permissible to exceed the yield limit. However, these areas must be small enough not to cause significant permanent deformations in the model when removed.

Additionally, it can be applied a ultimate failure criteria, following the same European standard as above. Equation 4.1.2 calculates the utilisation, which should also be less or equal to 1, with the new required safety margin, S_2, between the exceptional design load and the load causing structural failure.

$$U_2 = \frac{\sigma_c S_2}{R_m} \leq 1 \tag{4.1.2}$$

Where,

- U is the utilisation;
- R_m is the material ultimate stress (see table 3.2);
- σ_c is the calculated stress;
- S_2 is the safety factor.

When design verification relies solely on calculations, a safety factor of 1.5 is applied, as is the case in this analysis. Once again, if experimental tests confirm the numerical results, this safety factor can be reduced to 1.3.

Regarding deformations, EN 12663-2 [32] states that the maximum deflection of the underframe, under the normal design load, must not exceed 3 ‰ of the distance between bogie pivots from the initial position. This entails that, for this wagon, the maximum vertical displacement can not exceed 31.38 mm.

4.1.2 Results and discussion

This section will present the displacements and von Mises stress results for each load case. Ultimately, conclusions regarding structural compliance with the requirements will be drawn and summarised in table 4.1.

It is crucial to note that, throughout all analyses, the results obtained in the boundary conditions and load application points were intentionally excluded. This omission was made because these specific results do not portray the actual deformation of the structure in these regions, and their evaluation does not align with the objectives of this project, which are to study the general behaviour of the underframe. To address these aspects accurately, separate models with varying levels of detail would need to be examined.

- **HLC1 - Compressive force at buffer axis height**

The application of longitudinal compressive forces on the buffer axes induces compression throughout the structure, resulting in a horizontal maximum displacement of approximately -6.33 mm. In comparison to the overall dimensions of the underframe, these deformations can be considered negligible.

In addition to horizontal compression, these loads lead to vertical bending effects. This behaviour is depicted in figure 4.1, where a noticeable negative displacement of up to 8.49 mm is observed, occurring in the central area of the wagon. This evaluation of the vertical response is essential not only for identifying critical zones but also to ensure compliance with the maximum

deflection criterion, which has been set at 31.38 mm, as previously outlined in the methodology description.

Furthermore, this compression phenomenon results in a widening in the transverse direction of the region closest to the central articulation, coupled with torsional deformation of the lower part of the girder (illustrated in figure 4.2 by the z-component displacement plot).

Then, the von Mises stresses were extracted. The critical points are observed in the curved edges of the top plate near the inner coupling, reaching a maximum stress value of 266.21 MPa. The plot of these results can be observed in figure 4.3. These areas of higher stress occur due to the general compression of the structure, leading to the widening of that specific zone.

As previously stated, the results in the boundary conditions are excluded from the analysis. Nevertheless, it is essential to acknowledge the high stresses obtained in the areas of load application. This end section holds high importance in the underframe, as it carries the coupling mechanisms and transfers their loads. As it is, the model does not have much detail due to lack of information and measurements, and the results obtained may not be reliable due to local geometric non-linearities. Hence, further attention to this particular section is needed for future analysis, for example, by constructing local models to evaluate these details.

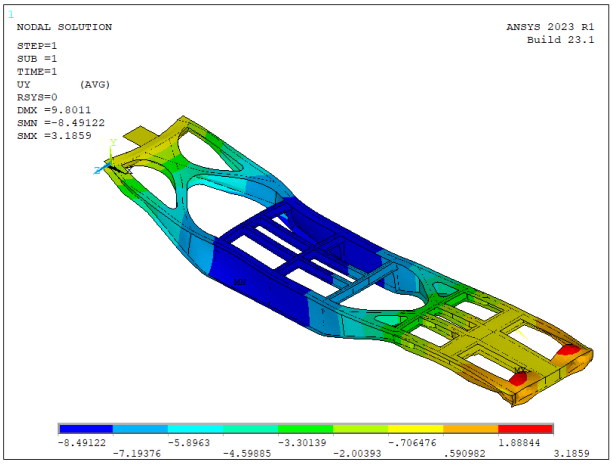

Figure 4.1: Vertical displacement plot for HLC1 (units in mm).

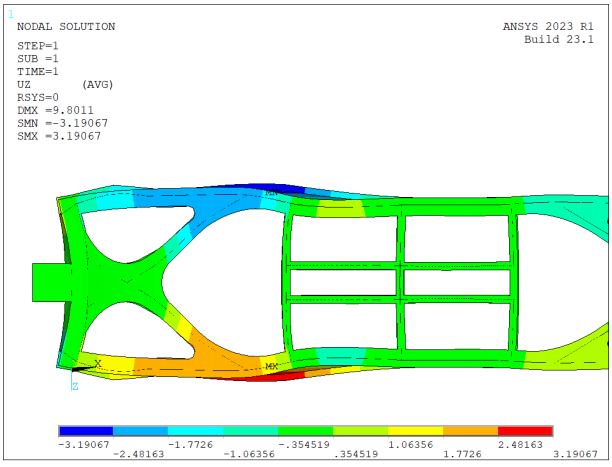

Figure 4.2: Transverse displacement plot for HLC1 (units in mm).

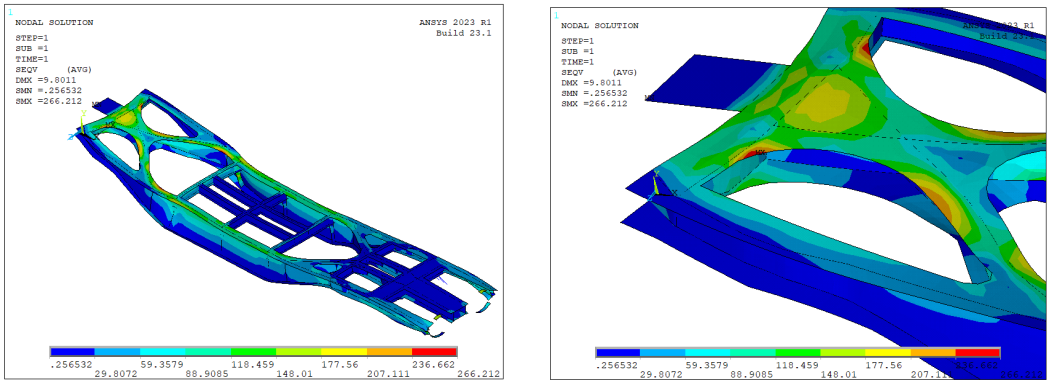

(a) Global perspective **(b)** Local perspective

Figure 4.3: von Mises stress plot for HLC1 (units in MPa).

- **HLC2 - Tensile force in coupler area**

The application of tensile forces to the structure results in a horizontal maximum displacement of approximately 6.66 mm. Once again, these deformations can be considered negligible relative to the overall dimensions of the underframe.

Moreover, under the influence of these forces, the structure experiences vertical flexural displacement, particularly in the central section, with a maximum positive displacement of 6.26 mm, as visually presented in figure 4.4. The analysis of this critical point concludes that the maximum displacement remains within the structural requirement boundaries, as specified by the relevant standard.

Interestingly, the deformation response of the structure under this load case showcases an opposite behaviour to the previous load case, which is consistent with the opposite nature of the applied forces. Consequently, the transverse displacement of the underframe exhibits a similar order of magnitude, but there is a noticeable narrowing of this section (as depicted in figure 4.5).

The distribution of von Mises stresses closely resembles the previous horizontal load case, as shown in figure 4.6. The highest stress recorded is 251.71 MPa. Once again, these high stress values are predominantly observed in the curved edges of the upper plate near the articulation.

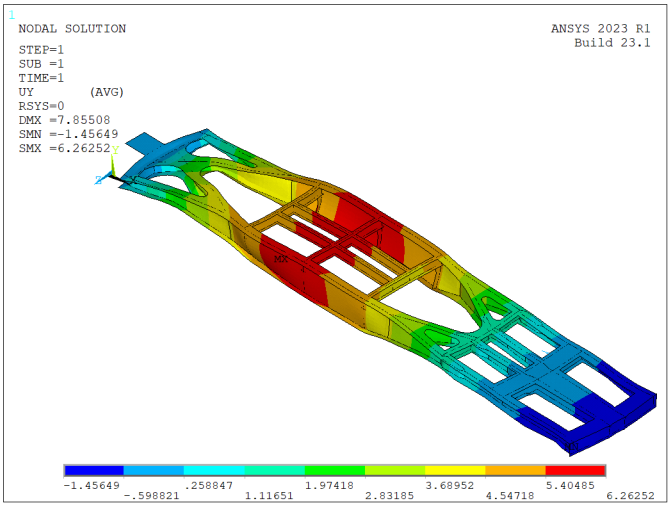

Figure 4.4: Vertical displacement plot for HLC2 (units in mm).

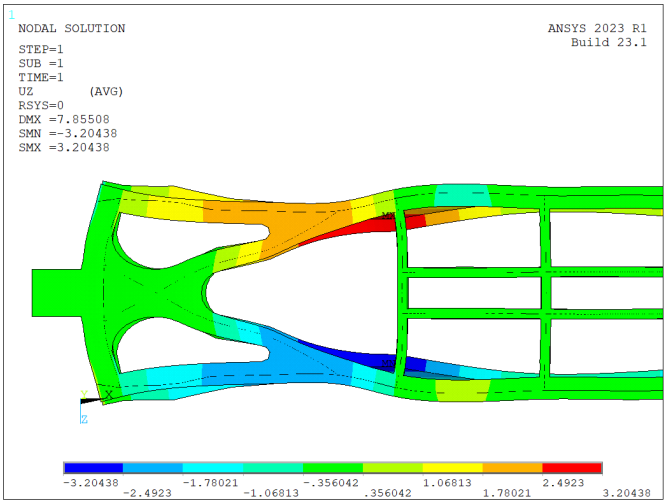

Figure 4.5: Transverse displacement plot for HLC2 (units in mm).

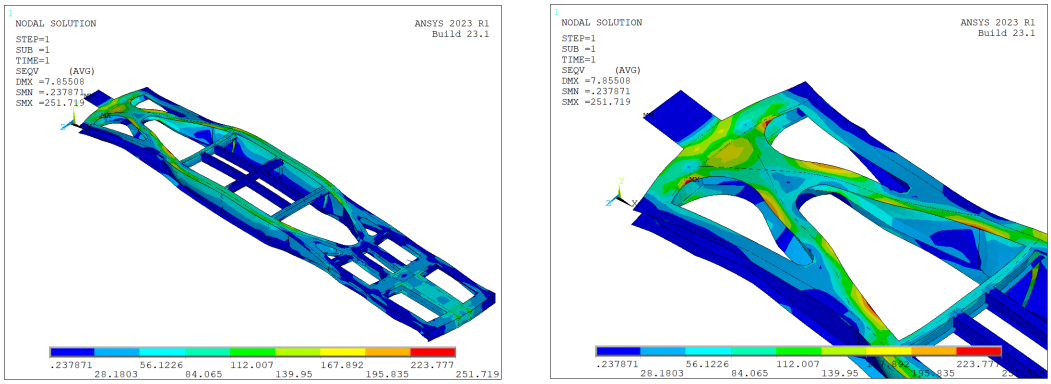

(a) Global perspective **(b)** Local perspective

Figure 4.6: von Mises stress plot for HLC2 (units in MPa).

- **VLC1 - Maximum operating load 40 ft container**

The structure exhibits significant bending deformation towards the rear end following the support of the bogie. The end section reaches a maximum vertical displacement of -24.69 mm, which is still below the deflection limit of 31.38 mm. This behaviour results from applying a substantial vertical force in the location of the spigot that supports the corner of the 40 ft wagon, which is located in an area with lower stiffness. In fact, the remaining structure experiences negligible deformations. Figure 4.7 shows the displacement results plot.

Concerning the stress distribution, the highest value recorded was 227.43 MPa in the upper plate corners, near the bogie region, as depicted in figure 4.8. These elevated values can be attributed to the substantial bending forces experienced in the vicinity of the supported area of the wagon. The central portion exhibits nearly negligible stress levels.

Within the boundary condition region of the bogie support, exceedingly high values are recorded (624.83 MPa), surpassing the material's yield limit. Although these values are not taken into account in this analysis, it becomes imperative to conduct a more detailed examination of the connection between the bogie and the underframe, thoroughly studying its behaviour and stresses.

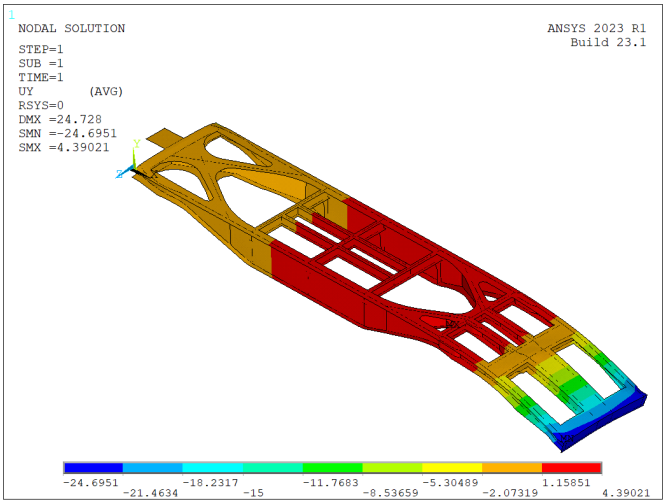

Figure 4.7: Vertical displacement plot for VLC1 (units in mm).

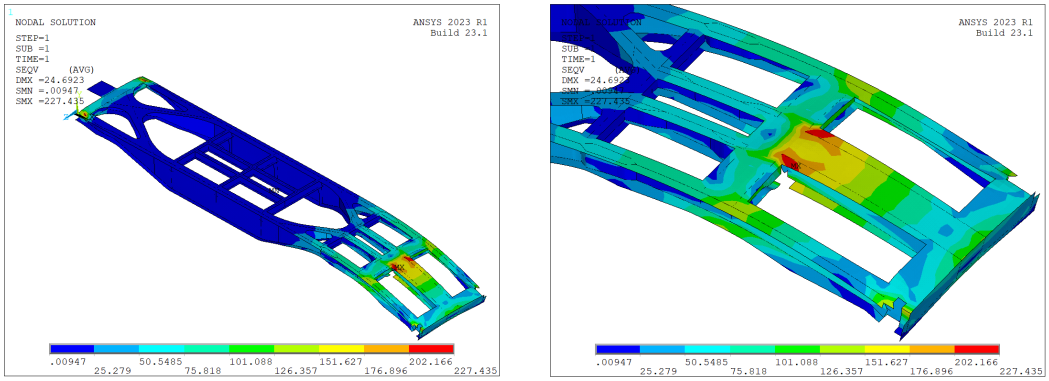

(a) Global perspective **(b)** Local perspective

Figure 4.8: von Mises stress plot for VLC1 (units in MPa).

- **VLC2 - Maximum operating load 2 x 20 ft containers**

The application of the load in the middle span of the longitudinal beam induces a bending effect in this unsupported section. The maximum displacement occurred precisely in this central area, measuring -12.66 mm, lower than the maximum deflection allowed of 31.38 mm. The plotted results are presented in figure 4.9.

Indeed, despite both vertical load cases having the same total load magnitude, there is a noticeable difference in how this load is distributed among the wagon. The central portion of the girder is loaded, contrary to the scenario of the 40 ft container, leading to the engagement of the maximum inertia of the beam and, due to the line of influence, causes a decrease in deformation towards the structure's ends. Additionally, the load applied in that final spigot is half of what is considered for the VLC1, further reducing the deformation of that area. This redistribution of load and its impact on the deformation characteristics of the underframe underscore the importance of considering load placement and distribution when analysing structural behaviour.

Figure 4.10 illustrates the Von Mises stress distribution. The maximum stress point occurs in the web of the girder near the load application. This result is due to the propagation of the stress concentrations that appear in the boundary condition. The web suffers compression and the critical point records a stress value of 235.59 MPa.

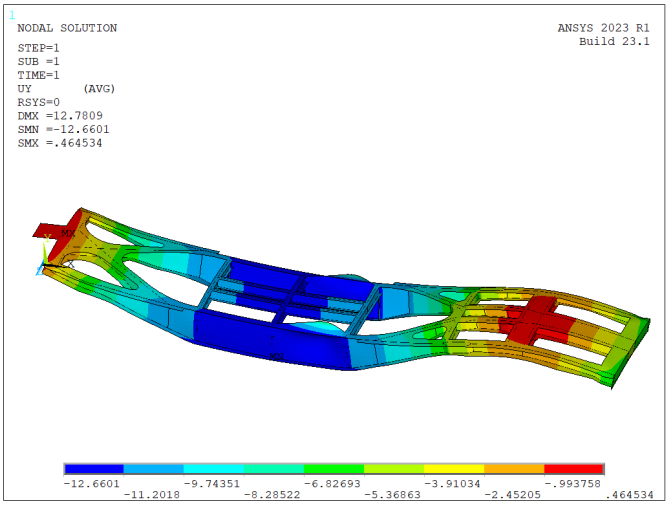

Figure 4.9: Vertical displacement plot for VLC2 (units in mm).

In the future, it would be important to carry out instability analyses. One example would be to investigate the possibility of buckling since compressive forces are acting on this beam web, which has a reduced thickness (around 8 mm).

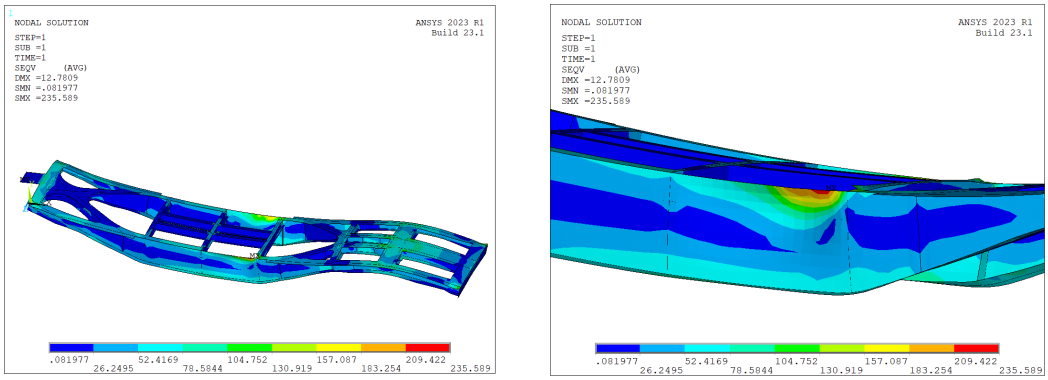

(a) Global perspective **(b)** Local perspective

Figure 4.10: von Mises stress plot for VLC2 (units in MPa).

It is worth noting that the top flange, where the load is applied, suffers large deflections (figure 4.11). In fact, the load application is not aligned with the core of the longitudinal beam, leading to the observed torsion effects in the upper flange. This simplified model does not contain the spigots and stiffeners aligned with these points, which help address the issues triggered by the load application. These two structures can be observed in figure 4.12.

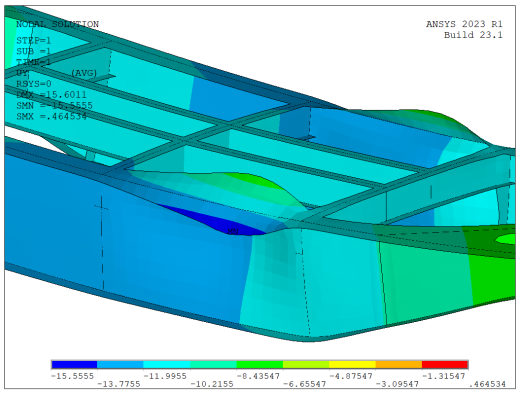

Figure 4.11: Deflection of top flange - VLC2.

Figure 4.12: Spigot and stiffener.

- **SLC1 - First superposition load case**

This load case combines the first horizontal load scenario involving compressive forces and the second vertical case (2 x 20ft containers), as can be consulted in table 3.3 in the subsection 3.3.6. It is evident that the results are a combination of the individual results already presented. The primary objective of these load cases is to analyse whether the superposition of the loads induces high stresses that could lead to structural failure.

The vertical displacement plot is presented in figure 4.13, where it is possible to observe that the maximum value is -16.65 mm in the middle section of the girder. Once again, this displacement does not exceed the maximum limit of 31.38 mm. The overlapping effect of the negative displacement from the two load cases is clear, producing a higher displacement in this situation than in the other two separate ones.

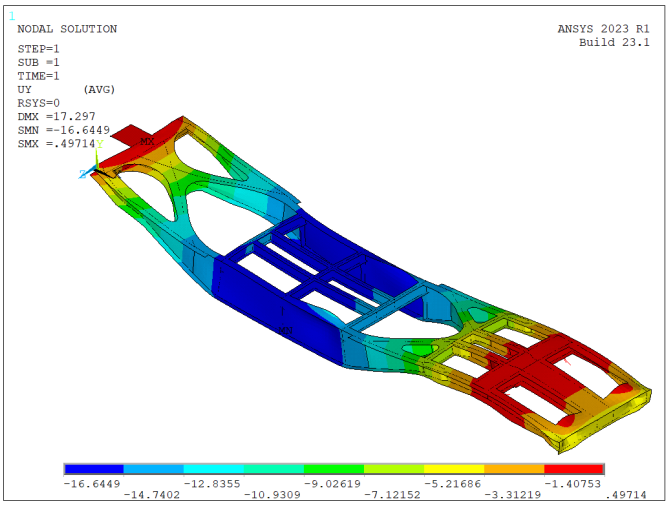

Figure 4.13: Vertical displacement plot for SLC1 (units in mm).

The maximum stress value is 300.34 MPa and appears in the curved edges of the top plate near the inner coupling, similar to the results produced by the horizontal load cases. The results plot is presented below in figure 4.14.

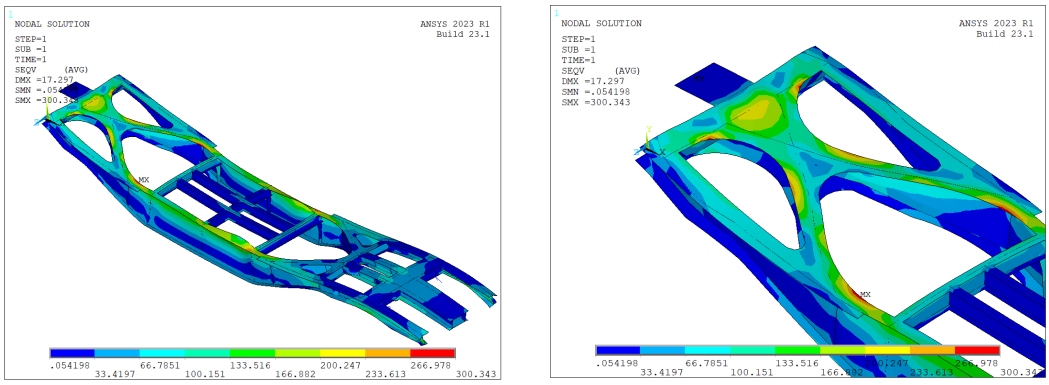

(a) Global perspective **(b)** Local perspective

Figure 4.14: von Mises stress plot for SLC1 (units in MPa).

- **SLC2 - Second superposition load case**

This load case results from the combination of the second horizontal load scenario, which involves tensile forces, and the second vertical case (2 x 20ft containers), as detailed in table 3.3 in subsection 3.3.6. It is evident that the outcomes are a synthesis of the previously presented individual results.

In this case, the largest vertical displacement is recorded at the rear of the wagon (-6.36 mm) because the horizontal tensile load induces a reverse bending effect compared to the vertical loads. In other words, the negative displacement is compensated. Where typically the largest deflection is observed, i.e., the central part of the wagon, the displacement is approximately half of that at the end of the wagon (-3 mm). This can be observed in figure 4.15.

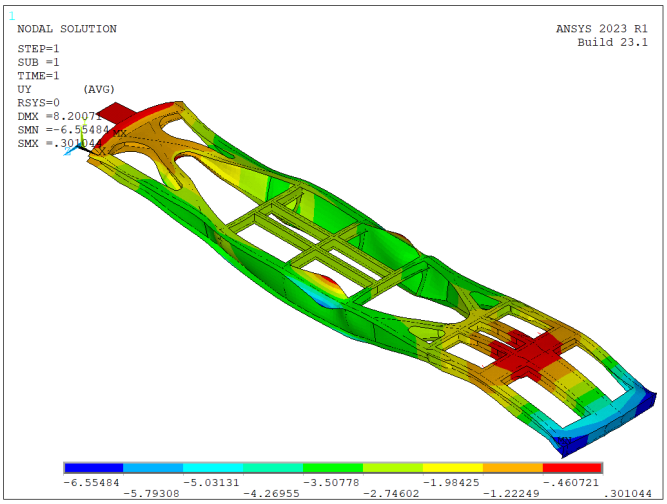

Figure 4.15: Vertical displacement plot for SLC2 (units in mm).

The stress distribution in the model is presented in figure 4.16. The maximum value obtained is 236.30 MPa, and this critical point is located, again, on the curved edge of the upper plate, as was previously observed in both horizontal load cases and the first superposition load case presented above.

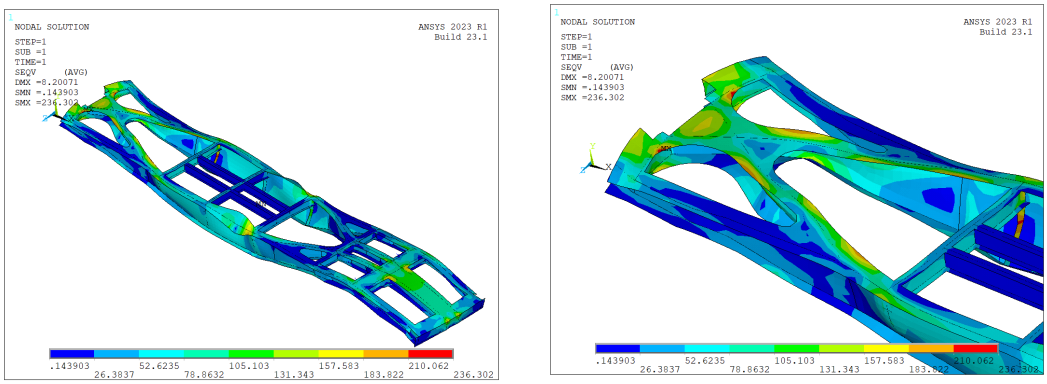

(a) Global perspective **(b)** Local perspective

Figure 4.16: von Mises stress plot for SLC2 (units in MPa).

4.1.3 Compliance Assessment

Finally, table 4.1 displays the maximum vertical displacements and maximum von Mises stress for each load case. The last two columns present the calculated yield or proof strength and ultimate failure utilisation parameters, with equations 4.1.1 and 4.1.2. These values must be less than or equal to 1 to satisfy the requirements. As observed in the table, all of them are below 1, confirming that the structure indeed meets these requirements.

The maximum deflection criterion mentioned in section 4.1.1 limits the maximum deformation to 31.38 mm. Comparing these results with the table, it becomes evident that no displacement exceeds the specified maximum limit, thus confirming compliance with this requirement.

Nonetheless, it should be highlighted that the maximum vertical displacement of the load case concerning the weight of the 40 ft container is relatively high. Delving further into the analysis of this structural area and, potentially, making geometric changes to enhance its stiffness could be beneficial. In fact, the modelling of this particular region raised several concerns due to a lack of measurements and information, as it involves enclosed and hard-to-access areas.

In conclusion, all imposed static criteria are met, and the structure complies with the standards.

Table 4.1: Results from static analysis.

Load Case	Vertical Displacement [mm]	σ_{VM} [MPa]	$U_1 \leq 1$	$U_2 \leq 1$
HLC1	−8.49	266.21	0.86	0.85
HLC2	6.26	251.71	0.82	0.80
VLC1	−24.69	227.44	0.74	0.73
VLC2	−12.66	235.59	0.76	0.75
SLC1	−16.65	300.34	0.97	0.96
SLC2	−6.36	236.30	0.77	0.75

4.2 Fatigue Analysis

Railway vehicle bodies endure a multitude of dynamic loads throughout their operational life, including those arising from loading/unloading operations and the track-induced forces, which are constantly changing. These loads predominantly impact specific critical elements within the structure, such as:

- Points of load application, including equipment attachments;
- Connections between structural components, such as welds and bolted joints;
- Changes in geometry that create stress concentration regions, like doors and window corners.

Identifying and addressing these critical features is paramount. It often requires a thorough examination of these localised elements to ensure structural integrity and safety. Moreover, the significance of conducting a fatigue analysis amplifies when considering the construction of the underframe, primarily comprised of welded plates and beam profiles. These welded regions are critical junctures in the wagon's structure, where the integrity of the welds is paramount for ensuring long-term performance and safety.

Below, the methodology applied to carry out this fatigue assessment is presented. Afterwards, the results for both vertical load cases are presented, followed by the study's conclusions.

4.2.1 Methodology

The approach to assessing fatigue relies on the results obtained from static simulations and extrapolating conclusions based on the guidelines presented in Eurocode 3 Part 1.9 [47]. The primary focus of this analysis will be on vertical load cases.

A crucial aspect to define is the dynamic load considered in this study. In this regard, the standard EN 12663-2 [32] stipulates that this load should fall within the range of ±30% of the vertical static load, following the cyclic stress plot in the shape of a sinus function, presented in figure 4.17.

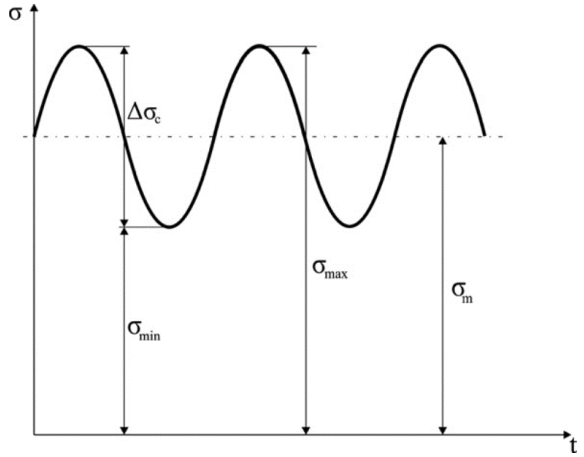

Figure 4.17: Sinusoidal loading for fatigue [48].

The equivalent constant amplitude stress range method is employed, guided by the S-N curve (also known as Wöhler's curve), illustrated in figure 4.18. In this context, fatigue is evaluated using the following equation 4.2.1:

$$\frac{\gamma_{Ff} \cdot \Delta\sigma_{E,2}}{\Delta\sigma_c/\gamma_{Mf}} \leq 1.0 \tag{4.2.1}$$

Where,

- γ_{Ff} is the partial factor for equivalent constant amplitude stress ranges;
- $\Delta\sigma_{E,2}$ is the equivalent constant amplitude stress range related to 2 million cycles;
- $\Delta\sigma_c$ is the reference value of the fatigue strength at $N_c = 2$ million cycles;
- γ_{Mf} is the partial factor for fatigue strength.

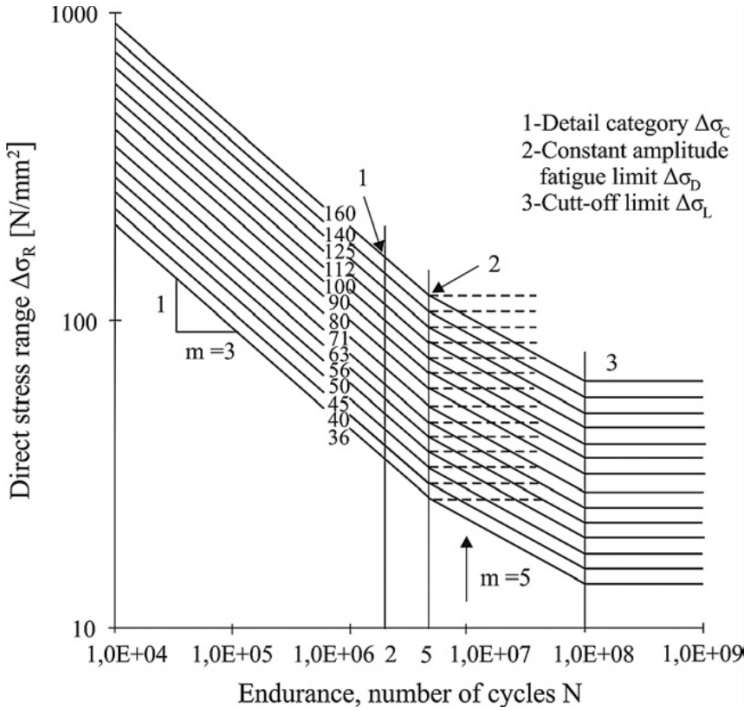

Figure 4.18: S-N curve (Wöhler's curve) [47].

The first factor, γ_{Ff}, is a safety coefficient for the fatigue action effect and is equal to 1. The other factor, γ_{Mf}, related with the fatigue strength, is recommended in relation to the chosen fatigue assessment philosophy, which are the following:

1. Damage tolerant method - allows initiation of cracks that do not affect the safety of the structure, given that periodic inspections and maintenance work are properly defined;
2. Safe life method - the component is designed with a fatigue life higher than its operation time, meaning that a detectable fracture must not initiate during its lifetime, and it is assumed that no regular inspections are mandatory.

The one employed in this analysis is the safe life method, consisting of a more conservative approach. The corresponding safety partial factors for fatigue strength for this philosophy, γ_{Mf}, are the following:

- Low consequence : $\gamma_{Mf} = 1.15$
- High consequence : $\gamma_{Mf} = 1.35$

Once again, keeping up with the conservative approach, it was determined to use the high consequence factor of 1.35.

The damage equivalent stress range, $\Delta\sigma_{E,2}$, is then calculated with equation 4.2.2 that estimates the equivalent stress for 2 million cycles.

$$\Delta\sigma_{E,2} = \lambda \cdot \Phi_2 \cdot \Delta\sigma \tag{4.2.2}$$

Where,

- λ is the damage equivalent factor and is equal to 1;
- Φ_2 is damage equivalent impact factor and is also equal to 1;
- $\Delta\sigma$ is the stress range of 60% retrieved from the finite element model.

Finally, the $\Delta\sigma_c$ values are the detail categories classified in tables 8.1 to 8.10 of the Eurocode 3 Part 1.9 [47]. These values depend on the details chosen to analyse, and the ones considered in this study are presented below.

Firstly, it will be evaluated the fatigue at parent material. For that, three different detail categories are considered (160, 140 and 125 MPa), as per table 8.1 of the standard. The purpose of these three categories is to evaluate the different scenarios dependent on the manufacturing process employed to fabricate the plates.

Next, in the vicinity of welded joints, three specific scenarios are taken into consideration. The first (Case 1) pertains to welding between the flanges and the web of a beam, with a detail category rating of 100 MPa. This corresponds to manual fillet welding, representing the worst case.

The second scenario (Case 2) involves butt welds between the flange plates, categorised at 80 MPa, which is the scenario with the lowest fatigue strength between these types of welds. This evaluation focuses on the girder, which predominantly employs this welding type, with plate thickness variations.

Lastly, the third scenario (Case 3) addresses the transverse butt welds at the intersecting flanges, carrying a detail category rating of 40 MPa. This case examines the connections between the girder and the transverse beams of the underframe.

Please refer to figure 4.19 for a visual representation of these three scenarios. It is important to note that the stress values obtained from the model correspond to the directional stress illustrated in the accompanying figures.

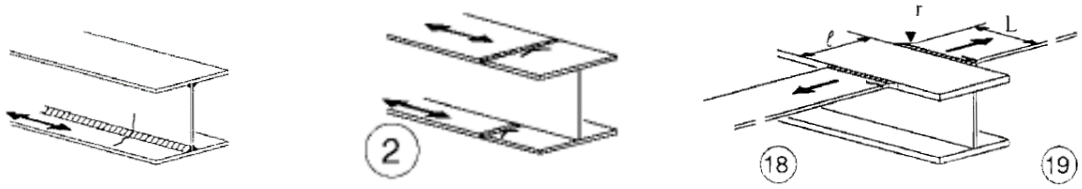

(a) Case 1 **(b)** Case 2 **(c)** Case 3

Figure 4.19: Welded joints scenarios [47].

4.2.2 Results and discussion

In terms of parent material zones, for VLC1, the maximum static stress in the longitudinal direction (σ_{xx}) is 231.50 MPa, located in the top plate near the bogie support (see figure 4.20). This specific stress point was already identified in the static analysis discussed in section 4.1. In the case of VLC2, the stress value is -139.99 MPa, indicating compressive stress. This value is recorded in the top flange of the girder, near the point of load application. This behaviour can be attributed to the bending response of the flange (see figure 4.21). The analysis of these results, utilising equation 4.2.1, is presented in table 4.2 for further evaluation.

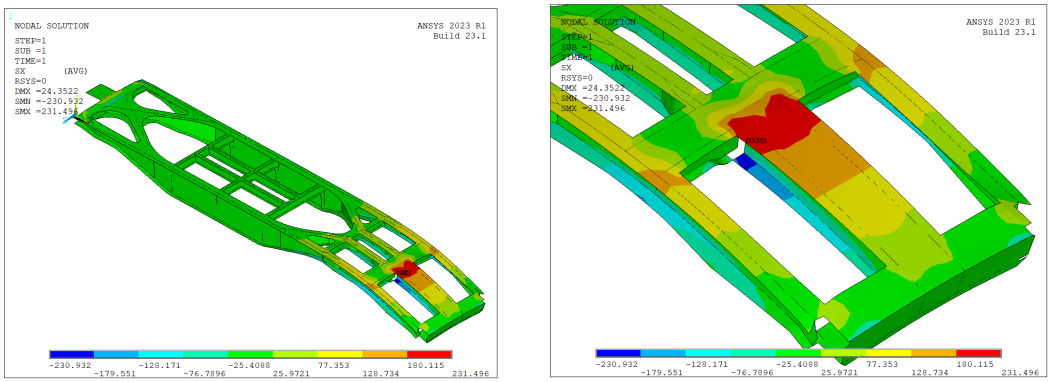

(a) Global perspective **(b)** Local perspective

Figure 4.20: Plot of x-component of stress - VLC1 (units in MPa).

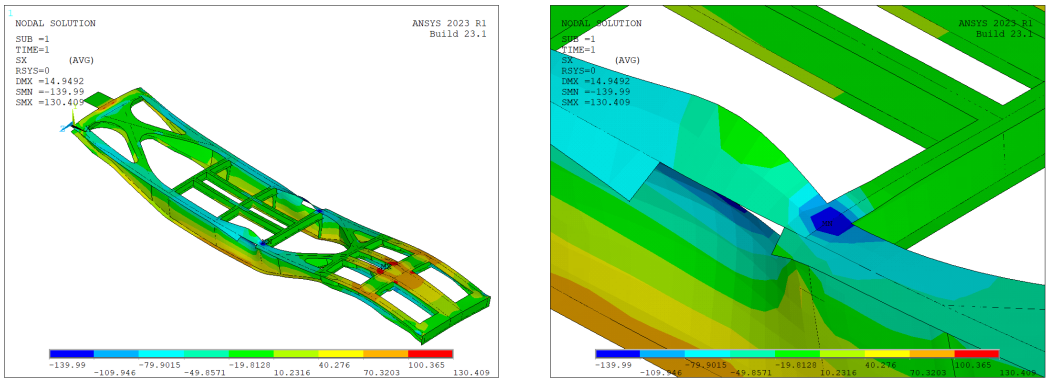

(a) Global perspective **(b)** Local perspective

Figure 4.21: Plot of x-component of stress - VLC2 (units in MPa).

Table 4.2: Fatigue results for parent material.

Load Case	Static Stress, σ_{xx} [MPa]	$\Delta\sigma_{E,2}$ (±30%) [MPa]	$\Delta\sigma_c$ (detail category) [MPa]	$\Delta\sigma_c/\gamma_{Mf}$ [MPa]	Eq. 4.2.1 (≤ 1)
VLC1	231.50	138.90	160.00	118.52	1.17
			140.00	103.70	1.34
			125.00	92.59	1.50
VLC2	-139.99	83.99	160.00	118.52	0.71
			140.00	103.70	0.81
			125.00	92.59	0.91

The primary conclusion drawn from these results is that the loading case involving the 40 ft container generates exceptionally high stresses that fail to meet the required fatigue criteria. Consequently, the wagon would experience structural failure before reaching its expected end-of-life. Interestingly, this specific region had already been identified as critical during the static analysis, even though it met the static requirements. The fatigue analysis reaffirms that this area is critical, emphasising the need for a more meticulous assessment and potential modifications to address this vulnerability.

Conversely, the other vertical loading case exhibits lower stress values and successfully meets the fatigue requirements. These results can be attributed to the distribution of the total load across more areas of the wagon, mitigating the risk of fatigue failure.

The secondary objective of the analysis was to evaluate the influence of plate manufacturing processes on fatigue response. However, definitive conclusions are challenging to draw. In the case of VLC1, failure occurs across all categories, while VLC2 satisfies the fatigue criteria for all of them. One suggestion that emerges is to ensure that plates are manufactured to the highest quality standards, ideally falling within the first category. This would reduce susceptibility to fatigue-related issues, although reevaluating the structure regarding these parameters remains necessary.

The underframe of the wagon is constructed through the welding of various plates and beams, making it crucial to assess the various welding scenarios incorporated into the model, as detailed in the methodology subsection. The results for the three welding scenarios under both load cases are summarised in table 4.3.

In the first fatigue case, for VLC1, the maximum stress σ_{xx} reached 221.42 MPa, occurring in the same critical region previously identified in the parent material analysis. Specifically, this stress was observed in the upper plate, near the bogie pivot point, as illustrated in Figure 4.20. For VLC2, the highest stress recorded was -149 MPa, localised at the connection of the web of the girder to the flange, near the load application point in the middle section of the girder. The stress distribution in the x direction is depicted in figure 4.22.

In the second welding case, the first load case recorded a stress of -82.18 MPa at the bottom flange of the girder. This stress concentration occurs at the welding bead between plates with different thicknesses after the bogie support section. In the second load case, the maximum stress reached 96.52 MPa, also on the bottom flange of the girder but closer to the start of the reduction of web height, on the side closer to the end of the wagon. Figure 4.23 and figure 4.24 present the stress distribution (σ_{xx}) for the first and second load cases, respectively.

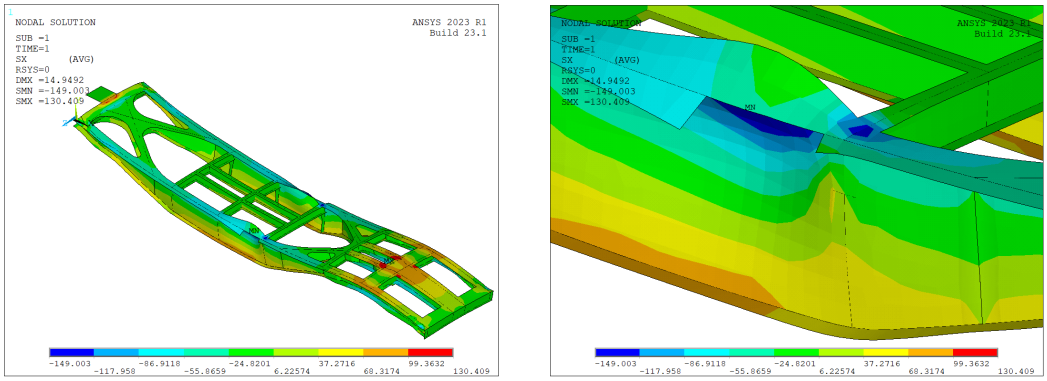

(a) Global perspective **(b)** Local perspective

Figure 4.22: Fatigue case 1: plot of x-component of stress - VLC2 (units in MPa).

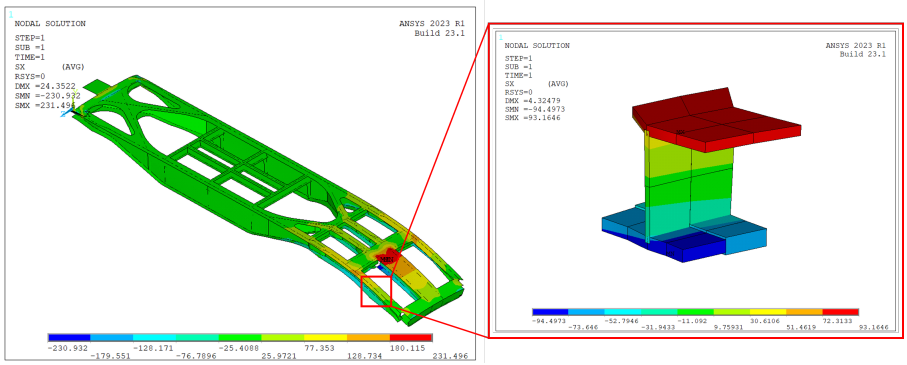

Figure 4.23: Fatigue case 2: plot of x-component of stress - VLC1 (units in MPa).

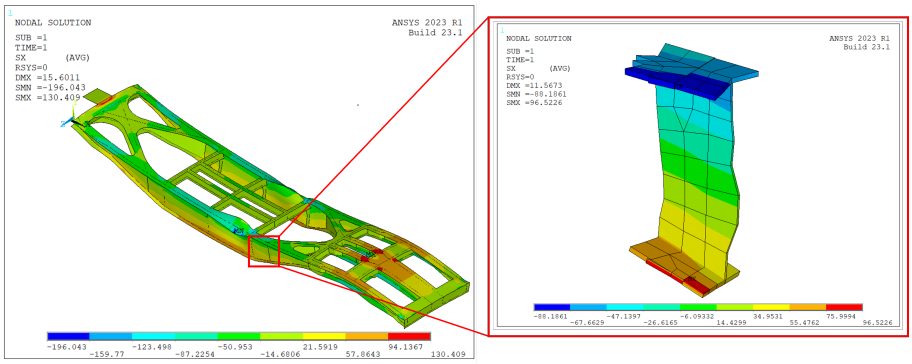

Figure 4.24: Fatigue case 2: plot of x-component of stress - VLC2 (units in MPa).

Finally, in the last welding case, the transverse stress component, σ_{zz}, is considered. In VLC1, the maximum value is 28.07 MPa, located in the connection zone between the girder and the transverse beam that connects to the bogie pivot (see figure 4.25). In VLC2, the maximum stress occurs in the connection between the girder and one of the normalised central I-beams (see figure 4.26), with a value of 55.01 MPa.

The results and their analysis for the three welding cases and the two load cases are summarised in table 4.3.

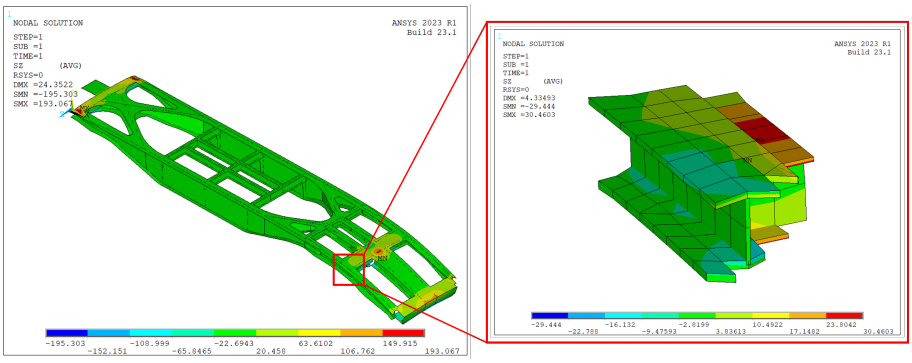

Figure 4.25: Fatigue case 3: plot of z-component of stress - VLC1 (units in MPa).

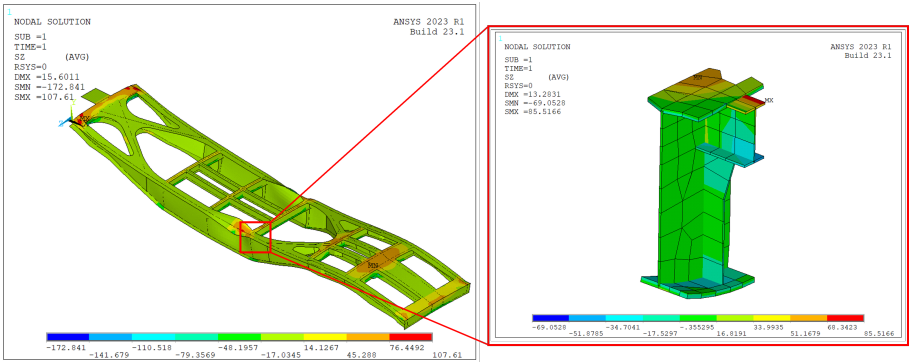

Figure 4.26: Fatigue case 3: plot of z-component of stress - VLC2 (units in MPa).

Table 4.3: Fatigue results in the vicinity of welded joints.

	Load Case	Static Stress [MPa]	$\Delta\sigma_{E,2}$ ($\pm$30%) [MPa]	$\Delta\sigma_c$ (detail category) [MPa]	$\Delta\sigma_c/\gamma_{Mf}$ [MPa]	Eq. 4.2.1 (≤ 1)
Case 1	VLC1	221.42	132.85	100.00	74.07	1.79
	VLC2	-149.00	89.40			1.21
Case 2	VLC1	-82.18	49.31	80.00	59.26	0.83
	VLC2	96.52	57.91			0.98
Case 3	VLC1	28.07	16.84	40.00	29.63	0.57
	VLC2	55.01	33.01			1.11

It is possible to observe that there are three scenarios in which the fatigue limit is exceeded. The first case (fatigue case 1 for VLC1) was expected since the maximum stress in the model resides in the same region, and the structure already failed to meet the fatigue requirements for the parent material. Likewise, for the same case but with VLC2, the static stresses exceeded the allowable limits for fatigue considerations. However, it is worth noting that this value was obtained from an area near the load application point, which raises some concerns about the reliability of these results. Similar concerns are raised for the last case that did not meet the requirements (case 3 for VLC2).

It is worth noting that these results were estimated using the detail category that would yield the worst-case scenario, ensuring a conservative approach. However, these findings underscore potential fatigue issues with the wagon's design.

This analysis has revealed particular fatigue-related challenges, emphasising the need for more

detailed investigations in the future. Specifically, constructing localised models to assess the behaviour of the structure and welds in greater depth is warranted. Additionally, gaining a more comprehensive understanding of the welds is essential for fine-tuning the detail category to be applied.

In conclusion, it is important to acknowledge that this model and analysis are in the preliminary stages. Identifying these critical areas provides valuable insights to guide further structural analysis and refine the wagon's design as it progresses towards its final form. Additionally, a less conservative and more precise fatigue analysis can be employed with the use of a damage accumulation approach with a loading spectra from literature or from measurements.

4.3 Modal Analysis

A modal analysis was performed to obtain the natural vibration frequencies and the respective mode shapes, allowing the dynamic characterisation of the structure and identification of its principal deformation behaviour. To this effect, the first eight mode shapes and frequencies were extracted from the finite element model and are listed in table 4.4 and presented in figure 4.27.

Table 4.4: Mode shapes and frequencies.

Mode No.	Frequency (Hz)	Description of mode shapes
1	17.75	1^{st} bending mode
2	19.59	1^{st} torsion mode
3	23.67	1^{st} lateral bending mode
4	31.95	2^{nd} lateral bending mode
5	32.41	2^{nd} bending mode
6	43.74	2^{nd} torsion mode
7	43.87	Lateral compression and torsion in girder
8	46.06	3^{rd} bending mode

The first vibration mode, characterised by a frequency of 17.75 Hz, corresponds to the primary vertical bending mode. This mode mainly influences the structure's response to symmetrical vertical loads. The second mode represents the first torsional mode, governing the response to asymmetric vertical loads, which introduce twisting forces into the structure. The third mode demonstrates a lateral bending behaviour of the wagon, related to shear loads, and it influences its response to lateral forces in the z-direction of the wagon. In the fourth mode, which also involves lateral bending, there is a notable deformation in the central section of the girder web, where the plate thickness is reduced. This localised deformation is significant for further structural analysis. The fifth vibration mode corresponds to the second vertical bending mode, revealing a substantial uplift at the end of the wagon. The sixth mode represents the second torsional mode, contributing to the structural torsional behaviour and helping assess how the wagon reacts to twisting forces. The seventh mode experiences tension in the longitudinal direction, leading to transverse compression and torsion in the girder, providing valuable insights into how the wagon responds to longitudinal loads. Lastly, the eighth mode represents the third vertical bending mode, shedding light on additional aspects of the structure's vertical flexural characteristics.

Collectively, these vibration modes provide a thorough insight into the dynamic behaviour of

the wagon when subjected to diverse loading conditions. This modal analysis is a foundational step for planning future dynamic and instability studies, thereby enriching the understanding on how the wagon responds to an array of dynamic loads and potential resonance scenarios. It is worth highlighting the importance of conducting a more in-depth examination of the girder, particularly focusing on the susceptibility of its web to deformations. This targeted investigation will help refine the wagon's structural design and enhance its overall performance by addressing specific areas of concern.

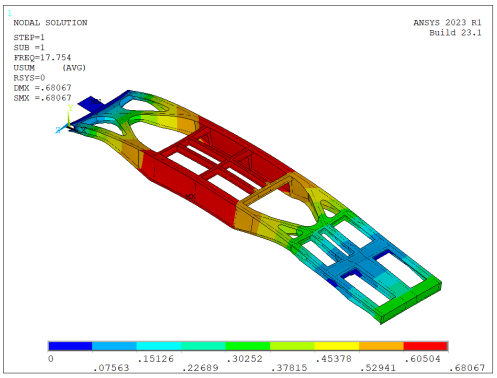

(a) First mode, $f = 17.75$ Hz

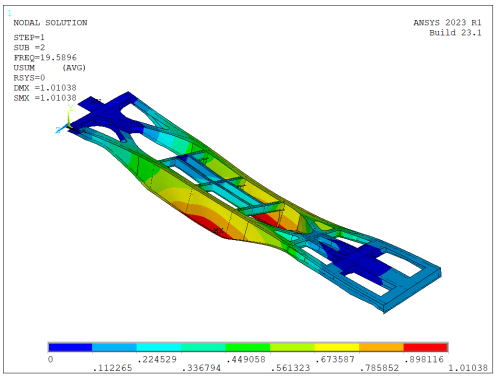

(b) Second mode, $f = 19.59$ Hz

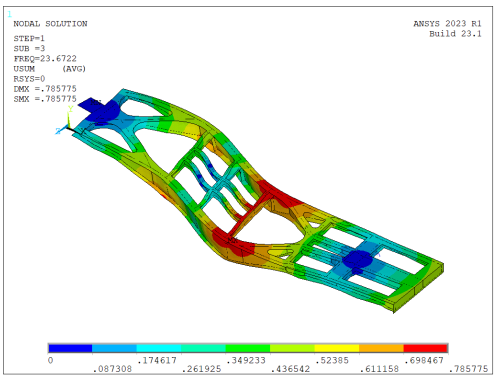

(c) Third mode, $f = 23.67$ Hz

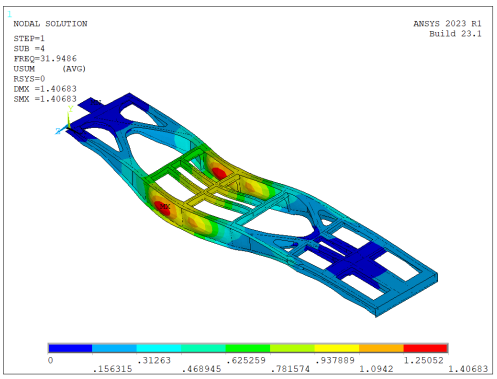

(d) Fourth mode, $f = 31.95$ Hz

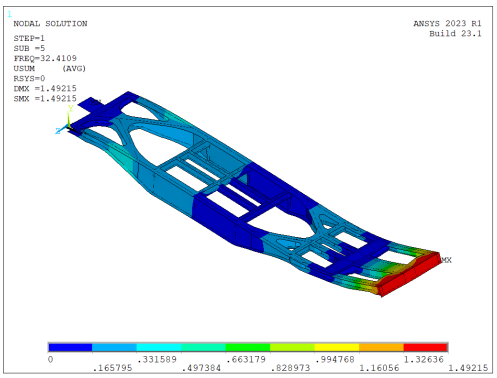

(e) Fifth mode, $f = 32.41$ Hz

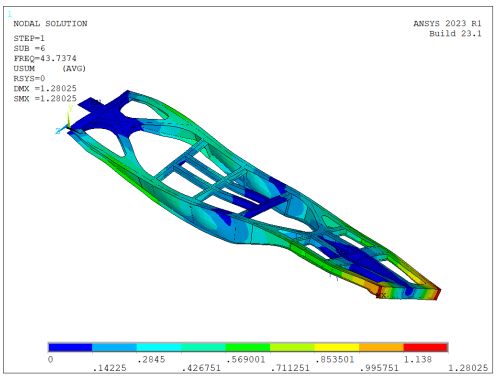

(f) Sixth mode, $f = 43.74$ Hz

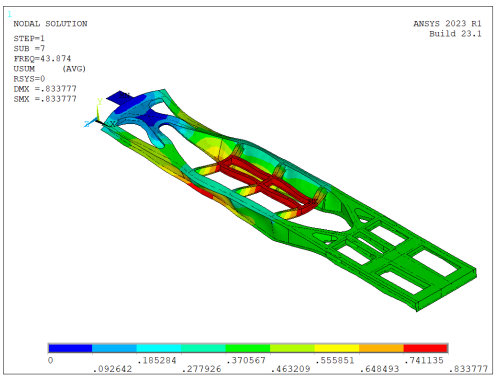

(g) Seventh mode, $f = 43.87$ Hz

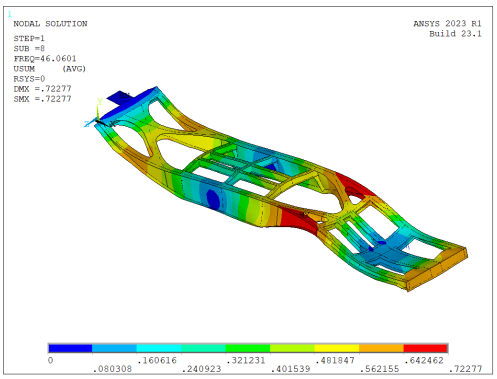

(h) Eighth mode, $f = 46.06$ Hz

Figure 4.27: Natural vibration modes.

Chapter 5

Conclusions and Future Work

This chapter describes the culmination of the work carried out in this dissertation, drawing conclusive findings from the structural analysis conducted. It is essential to highlight that this work represents the initial phase of the Smart Wagons project, thus opening up numerous avenues for more detailed analysis and exploration in the future.

5.1 Concluding Remarks

The primary objective of this dissertation was to create a geometric model of the Sggrss 80', 6-axle articulated intermodal wagon and subject it to a rigorous structural analysis. A meticulously crafted finite element model (FEM) was developed, with careful consideration given to mesh definition, and the boundary conditions pertaining to the wagon's connection to the bogie and the central articulation were applied thoughtfully. Six distinct load cases were simulated in order to comply with existing standards, encompassing horizontal compression on buffers, horizontal tension on the coupling system, vertical forces associated with the loading of a 40 ft container or two 20 ft containers, and two cases involving the superposition of horizontal and vertical loads.

Results were extracted and evaluated for static, fatigue, and modal analysis. The key findings are outlined below:

- The wagon complies with static structural requirements prescribed by the relevant standards. Notably, concerning vertical displacements, the most critical case is VLC1, corresponding to the 40 ft container scenario, exhibiting a maximum deformation of -25 mm at the wagon's extremity. Regarding stresses, SLC1, the superposition of horizontal compression and vertical loading, yields the highest value, reaching 300 MPa at the curved edges of the top plate near the inner coupling.
- It is imperative to note that this assessment did not consider boundary condition local stress/deformation values. Nevertheless, instances of high stress concentrations were detected, underscoring the need for careful attention in future, using more specialized local analyses.
- Conversely, the fatigue analysis raised concerns regarding compliance. Presently, this model is not certified for fatigue-related issues. Stresses obtained for the parent material in VLC1 exceeded permissible limits. In the analysis of welded joints, for Case 1 (the connection between the flange and the web of a beam), both loading scenarios resulted in failure. Cases

2 and 3 were only examined in the girder. No failure occurred for Case 2 involving a transverse butt weld in the flange. However, for Case 3, transverse butt welding at intersecting flanges, VLC2 exhibited stress levels surpassing allowable limits.

- Lastly, the modal analysis enabled the identification of natural frequencies and vibration modes. The first mode corresponds to the first bending mode, with a frequency of 17.75 Hz, indicating substantial underframe stiffness.

5.2 Future Work

As this work serves as an initial stepping stone in the Smart Wagons project, numerous areas warrant further improvement and in-depth exploration in the future. While several of these areas have been highlighted throughout this document, the following points stand out:

Geometric Model Refinement

The current geometric model includes certain simplifications and uncertainties. These aspects need addressing for a more accurate representation of the real-world wagon. Specific areas for improvement encompass the transverse beam where the bogie attaches, the wagon's extremities, and the central articulation zone.

Complete Load Cases Analysis

The EN 12663-2 standard defines several load cases for testing, and not all of them were considered in this study. Future endeavours should encompass these omitted cases.

Element Type Investigation

The FEM simulation employed shell elements. Investigating whether solid elements would yield more accurate results would be valuable.

Boundary Conditions Scrutiny

Boundary conditions consistently posed challenges in simulations. Although not considered for requirements verification, they remain critical aspects that require detailed assessment. Creating more detailed local models, for instance, could be beneficial.

Advanced Fatigue Analysis

In fatigue analysis, a simplified methodology was applied. Employing more rigorous and precise analyses, such as creating local models to assess fatigue in welding zones, would be intriguing, as well as using a damage accumulation approach with a stress spectra representative of real operation.

Topology Optimization

Not addressed in this thesis is topological optimization. After these initial analyses, it would be possible to evaluate the impact of design alterations for mass reduction without compromising structural stability.

Stability Analysis

Lastly, but certainly not of lesser importance, stability analyses are pivotal for vehicle performance. After the analyses presented here and identifying potential weak points, it is crucial

to conduct an stability analysis, for instance, of the longitudinal beam's web. These considerations are highly relevant to the topology optimization process, aiming to avoid local or global buckling.

References

[1] Janša J. Rail transport should once again become a driver of development - EU monitor. 2021. URL: https://www.eumonitor.eu/9353000/1/j9vvik7m1c3gyxp/vlnm7e90wzxe?ctx=vg9pkzu1yryd&tab=1; [Online; accessed 2023-05-17].

[2] CO2 emissions from cars: facts and figures (infographics). News | European Parliament 2021;URL: https://www.europarl.europa.eu/news/en/headlines/society/20190313ST031218/co2-emissions-from-cars-facts-and-figures-infographics; [Online; accessed 2023-05-17].

[3] European Comission . Climate Action. Transport emissions. 2019,.

[4] European Comission . The Core Network Corridors: Trans European Transport Network 2013. 2013,.

[5] European Union . Decision of the Adoption of the Shift2Rail Master Plan. Report: Strategic Masterplan. 2015,.

[6] Iwnicki S, Spiryagin M, Cole C, McSweeney T, editors. Handbook of Railway Vehicle Dynamics. CRC Press; 2019. ISBN 9780429469398. doi:10.1201/9780429469398.

[7] European Committee for Standardization . EN 15273-1: Railway applications - Gauges - Part 1: General - Common rules for infrastructure and rolling stock. 2013.

[8] Commission regulation (eu) 2015/995 of 8 june 2015 amending decision 2012/757/eu concerning the technical specification for interoperability relating to the 'operation and traffic management' subsystem of the rail system in the european union. Official Journal of the European Union; 2015. URL: https://eur-lex.europa.eu/legal-content/EN/TXT/?uri=CELEX%3A32015L0995.

[9] Krishna V, Stichel S, Henning A, Tarajcak P. Development of Functional Requirements for Sustainable and Attractive European Rail Freight. Deliverable 4.1 - State of the Art. Report of project FR8RAIL; 2017.

[10] Category: Covered railway wagons of the Netherlands. 2013. URL: https://commons.wikimedia.org/wiki/Category:Covered_railway_wagons_of_the_Netherlands; [Online; accessed 2023-06-05].

[11] Fartan M, Ulianov C. Innovative Monitoring and Predictive Maintenance Solutions on Lightweight Wagon - Deliverable D3.1-Freight vehicle lightwight concept design. Report of project INNOWAG; 2018.

[12] Revolution Trains . TEA tank wagon. 2017. URL: https://revolutiontrains.com/tea-wagon-project/; [Online; accessed 2023-06-05].

References

[13] Greenbrier Europe . Hopper wagons. 2022. URL: https://www.greenbrier-europe.com/category/products/hopper-wagons/page/3/; [Online; accessed 2023-06-05].

[14] Spiryagin M, Cole C, Sun YQ, McClanachan M, Spiryagin V, McSweeney T. Design and Simulation of Rail Vehicles. CRC Press; 2014. ISBN 9781466575677. doi:10.1201/b17029.

[15] Agico Group . Freight Wagon Wheelset. 2021. URL: https://railwaywagons.com/components-parts/wheelset/; [Online; accessed 2023-06-18].

[16] Jönsson PA. Freight wagon running gear–a review. TRITA–FKT Report 2002;35.

[17] Dias D. Bogie inteligente. Master's thesis; Faculdade de Engenharia da Universidade do Porto; Porto; 2008.

[18] SKF . Railway Technical Handbook: A Handbook for the Industrial Designer and Operator. Axleboxes, wheelset bearings, sensors, condition monitoring, subsystems and services. Sweden; 2011. ISBN 9789197896634.

[19] Iwnicki SD, Stichel S, Orlova A, Hecht M. Dynamics of railway freight vehicles. Vehicle System Dynamics 2015;53:995–1033. doi:10.1080/00423114.2015.1037773.

[20] Orvnas A, hogskolan. Jarnvagsgruppen. KT. Methods for reducing vertical carbody vibrations of a rail vehicle : a literature survey. KTH Railway Group; 2010. ISBN 9789174156317.

[21] European Committee for Standardization . EN 16235: Railway application - Testing for the acceptance of running characteristics of railway vehicles - Freight wagons - Conditions for dispensation of freight wagons with defined characteristics from on-track tests according to EN 14363. 2013.

[22] Sunbuloglu E, Bozdag E. A design strategy on the talbot type articulation of a freight wagon. WIT Transactions on the Built Environment 2018;181:145–56. doi:10.2495/CR180131.

[23] WAG-TSI. Commission Regulation (EU) No 321/2013 (13 Mar. 2013), amended by Commission Regulation (EU) No 1236/2013 (2 Dec. 2013) and Commission Regulation (EU) 2015/924 (8 Jun. 2015). 2013.

[24] Milovanović V, Zivković M, Disić A, Rakić D, Zivković J. Experimental and numerical strength analysis of wagon for transporting bulk material. IMK-14-Istraživanje i razvoj 2014;20(2):61–6.

[25] Šťastniak P, Moravčík M, Smetanka L. Investigation of strength conditions of the new wagon prototype type Zans. MATEC Web of Conferences 2019;254:02037. doi:10.1051/matecconf/201925402037.

[26] Stoilov V, Simić G, Purgić S, Milković D, Slavchev S, Radulović S, et al. Comparative analysis of the results of theoretical and experimental studies of freight wagon sdggmrss-twin. IOP Conference Series: Materials Science and Engineering 2019;664. doi:10.1088/1757-899X/664/1/012026.

[27] Orlova A, Keschwari SM, Cosic KA, Jönsson PA, Stichel S, Hermann KT, et al. The sustainable freight railway: Designing the freight vehicle-track system for higher delivered tonnage with improved availability at reduced cost - Deliverable 3.7 "A DESIGN GUIDE FOR SUSTAINABLE FREIGHT VEHICLES". Report of project Sustrail; 2015.

[28] Płaczek M, Wróbel A, Baier A. Computer-aided strength analysis of the modernized freight wagon. IOP Conference Series: Materials Science and Engineering 2015;95. doi:10.1088/1757-899X/95/1/012042.

[29] Krason W, Niezgoda T. FE numerical tests of railway wagon for intermodal transport according to PN-EU standards. Bulletin of the Polish Academy of Sciences: Technical Sciences 2014;62:843–51. doi:10.2478/bpasts-2014-0093.

[30] Šťastniak P, Kurčík P, Pavlík A. Design of a new railway wagon for intermodal transport with the adaptable loading platform. MATEC Web Conf 2018;235:00030. doi:10.1051/matecconf/20182.

[31] Slavchev S, Georgieva K, Stoilov V, Purgic S. Analysis of the results of theoretical and experimental studies of freight wagon Fals. Facta Universitatis, Series: Mechanical Engineering 2015;13:91–8.

[32] European Committee for Standardization . EN 12663-2: Railway applications – Structural requirements of railway vehicle bodies – Part 2: Freight wagons. 2010.

[33] European Committee for Standardization . EN 15566: Railway applications - Railway Rolling stock - Draw gear and screw coupling. 2022.

[34] European Committee for Standardization . EN 16019: Railway applications - Automatic coupler - Performance requirements, specific interface geometry and test method. 2014.

[35] European Committee for Standardization . EN 15551: Railway applications - Railway rolling stock - Buffers. 2022.

[36] European Committee for Standardization . EN 15085: Railway applications - Welding of railway vehicles and components. 2007.

[37] European Committee for Standardization . prEN 17149: Railway applications - Strength assessment of railway vehicle structures. 2021.

[38] Greenbrier Europe . Sggrss 80' | 6-axle articulated intermodal wagon. 2022. URL: https://www.greenbrier-europe.com/2022/10/08/sggrss-80-6-axle-articulated-intermodal-wagon/; [Online; accessed 2023-07-29].

[39] European Committee for Standardization . EN 10025-3: Hot rolled products of structural steels - Part 3: Technical delivery conditions for normalized/normalized rolled weldable fine grain structural steels. 2004.

[40] SHELL 181. 2017. URL: https://www.mm.bme.hu/~{}gyebro/files/ans_{}help_{}v182/ans_{}elem/Hlp_{}E_{}SHELL181.html; [Online; accessed 2023-07-20].

[41] Opala M. Evaluation of bogie centre bowl friction models in the context of safety against derailment simulation predictions. Archive of Applied Mechanics 2018;88:943–53. URL: https://doi.org/10.1007/s00419-018-1351-4. doi:10.1007/s00419-018-1351-4.

[42] Wagon Stresses. UIC Code: 577; 1991. International Union of Railways.

[43] Slavchev S, Stoilov V, Purgic S. Static strength analysis of the body of a wagon, series Zans. Journal of the Balkan Tribological Association Vol 2015;21(1):38–57.

[44] Talleres Alegría, s.a. . Container Wagon Sggrss 80' Catalog; n.d.

[45] Standard wagons - Wagons for combined transport - Characteristics. UIC Code: 571-4; 2011. International Union of Railways.

[46] European Committee for Standardization . EN 12663-1: Railway applications – Structural requirements of railway vehicle bodies - Part 1: Locomotives and passenger rolling stock (and alternative method for freight wagons). 2010.

References

[47] European Committee for Standardization (CEN) . Eurocode 3 - Design of steel structures, Part 1-9: Fatigue. Brussels, Belgium: European Committee for Standardization (CEN); 2005.

[48] Milovanović V, Dunić V, Rakić D, Živković M. Identification causes of cracking on the underframe of wagon for containers transportation - fatigue strength assessment of wagon welded joints. Engineering Failure Analysis 2013;31:118–31. doi:10.1016/j.engfailanal.2013.01.039.